We are IntechOpen,
the world's leading publisher of
Open Access books
Built by scientists, for scientists

6,900
Open access books available

186,000
International authors and editors

200M
Downloads

154
Countries delivered to

Our authors are among the

TOP 1%
most cited scientists

12.2%
Contributors from top 500 universities

BOOK CITATION INDEX
CLARIVATE ANALYTICS
INDEXED

WEB OF SCIENCE™

Selection of our books indexed in the Book Citation Index
in Web of Science™ Core Collection (BKCI)

Interested in publishing with us?
Contact book.department@intechopen.com

Numbers displayed above are based on latest data collected.
For more information visit www.intechopen.com

Improved Power Quality AC/DC Converters

Abdul Hamid Bhat and Pramod Agarwal
National Institute of Technology Srinagar, Kashmir
India

1. Introduction

In this chapter, various power quality problems created by the widespread use of conventional diode bridge rectifiers and line-commutated AC/DC converters have been discussed. The impact of these problems on the health of power systems and working of sensitive equipments has also been discussed. Need for addressing these burning power quality issues has been emphasized. Recent trends of addressing these issues have been briefly discussed. A new breed of improved power quality AC/DC converters has been discussed in details. Development of various topologies and state-of-art of this breed of converters has been discussed briefly. The state-of-the-art multilevel converters used as improved power quality converters have been covered in this chapter with emphasis on three-level neutral-point clamped converters. This converter has been investigated for improved power quality and various simulation results have been presented to prove their effectiveness in terms of excellent power quality like nearly unity input power factor and negligible harmonic distortion of source current. The simulation results have been obtained with sinusoidal PWM and sapce-vector PWM modualtion algorithms. Simulation restls have been validated through experimental results which are obtained on a three-level converter by real-time implementation of space-vector PWM technique using a real-time DSP board. The performance investigation of the converter proves the effectiveness of three-level converter in elegantly addressing the burning power quality issues.   We know that power systems are designed to operate at frequencies of 50 or 60 Hz. However, certain types of loads produce harmonic currents in the power system. The power system harmonics are not a new phenomenon. Concern over harmonic distortions has ebbed and flowed during the history of electrical power systems. Traditionally the saturated iron in transformers and induction machines, electric arc furnaces, welding equipment, fluorescent lamps (with magnetic ballasts), etc. have been responsible for the generation of harmonics in electric power systems. Most of these equipments also cause the flow of reactive component of current in the system. In recent years, many power electronic converters utilizing switching devices are being widely used in domestic, commercial and industrial applications, ranging from few watts to MWs. However these converters suffer from the drawbacks of harmonic generation and reactive power flow from the source and offer highly non-linear characteristics. The generation of harmonics and reactive power flow in the power systems has given rise to the 'Electric Power Quality' problems. Any significant deviation in the magnitude of the voltage, current and frequency, or their waveform purity may result in a

potential power quality problem. Power quality problems arise when these deviations exceed beyond the tolerable limit and can occur in three different ways as frequency events, voltage events and waveform events. Distortion of the voltage/current waveforms from the normal sinusoidal waveshape is considered as waveform event. *One of the most harmful waveform events are the harmonic distortions. Harmonics are basically the additional frequency components present in the mains voltage or current which are integer multiples of the mains (fundamental) frequency. Harmonic distortion originates due to the nonlinear characteristics of devices and loads on the power system.* The inter-harmonics are due to the presence of additional frequencies which are non-integral multiples of the mains frequency. Moreover, notching is a periodic voltage disturbance caused by the normal operation of power electronic devices when current is commutated from one phase to another.

All these disturbances may originate problems to both utility and customers. Among them, harmonic distortions are considered one of the most significant reasons for power quality problems. Harmonic problems counter many of the conventional rules of the power system design and operation that consider only the fundamental frequency. Harmonic distortions are mainly caused by the nonlinear devices in which the current is not proportional to the applied voltage as shown in Fig. 1, where a nonlinear resistor is supplied by a sinusoidal voltage source. The resulting current is distorted while the applied voltage is perfectly sinusoidal. Increasing the voltage by a few percent may cause the current to double and take a different waveshape. This, in essence, is the source of harmonic distortion in the power system.
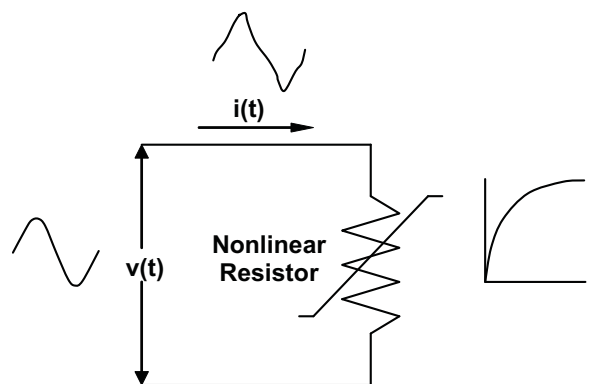

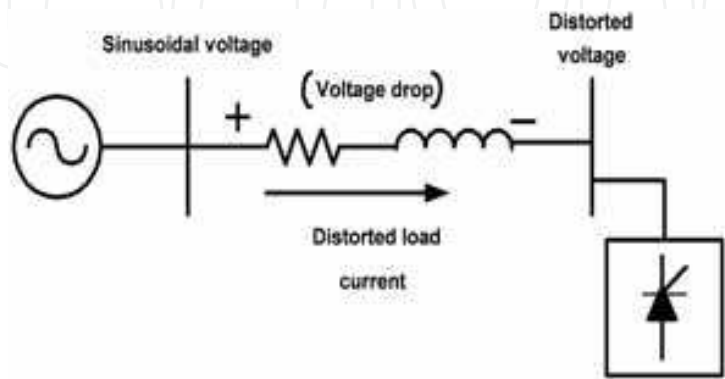Fig. 1. Current distortion caused by nonlinear resistor

Fig. 2. Distorted voltage at load bus caused by harmonic current flow through the system impedance

2. Causes and effects of harmonics and reactive power

Any device with nonlinear characteristics that derives input power from a sinusoidal electrical system may be responsible for injecting harmonic currents and voltages into the electrical power system. Developments in digital electronics and power semiconducting devices have led to a rapid increase in the use of nonlinear devices. Power converters, most widely used in industrial, commercial and domestic applications are considered the primary source of undesired harmonics. In converter theory, the DC current is considered to be constant and the line currents at the AC side will consist of abrupt pulses instead of a smooth sinusoidal wave. Power, the product of voltage and current, at the DC side contains harmonics in the current/voltage. Since no energy storage can take place in the elements of a converter, the power balance of the input and output requires harmonics in the input power, and thus harmonic currents will flow in the supply lines. Energy balance considerations show and Fourier analysis of the square waves confirm that for a 6-pulse converter, each 6n harmonics in the DC voltage requires harmonic currents of frequencies 6n±1 in the AC lines. Harmonics are the integral multiples of fundamental frequency superimposed on the fundamental frequency. These harmonics combine with the fundamental to form distorted waveshapes.

Harmonics are caused by the loads in which the current waveform does not conform to the fundamental waveform of the supply voltage. These loads are called the nonlinear loads and are the source of harmonic current and voltage distortion. Current harmonics generated by these nonlinear loads are propagated throughout the power network. Voltage distortion is the result of these distorted currents passing through the series impedance of the system, as shown in Fig. 2. Harmonic current passing through the system impedance causes a voltage drop for each harmonic and results in voltage harmonics appearing at the load bus and leads to power quality problems. The most common measure of distortion is the total harmonic distortion, THD. THD applies to both current and voltage and is defined as the rms value of harmonics divided by the rms value of the fundamental, multiplied by 100. THD of current varies from a few percent to more than 100%. THD of voltage is usually less than 5% but values above 10% are definitely unacceptable and cause problems for the sensitive equipment and loads. Most of the power electronic loads include AC/DC converters which are the primary source of harmonics and reactive power flow in a power system.

Some of the commonly used AC/DC converters have been simulated using MATLAB/Simulink software. The waveforms of source voltage and source current in all the cases have been plotted and the harmonic spectrum of source current in all the cases has been obtained to prove the power quality problems (like injection of harmonics in source current and deterioration of input power factor) created by these converters. Fig. 3 depicts the load voltage and load current waveforms of a single-phase diode bridge rectifier driving an R-L load. Fig. 4 shows the corresponding source voltage and source current waveforms. It can be clearly seen from the harmonic spectrum of source current in Fig. 5 that the source current in highly distorted with a THD of about 43%. Fig. 6 shows the waveforms of source voltage and source current drawn by a single-phase practical bridge rectifier with a filter capacitor connected across the load and Fig. 7 shows the corrrsponding harmonic spectrum of the source current which shows the THD of source current as high as 54.24%. Fig. 8 shows the waveforms for source voltage and source current for a single-phase fully-controlled converter driving an R-L load at a firing angle of 90° and Fig. 9 shows source current harmonic spectrum with a THD of 54.25%. Fig. 10 shows the phase *A* source voltage and source current waveforms for a three-phase fully-controlled converter driving an R-L

load at a firing angle of 90°. Fig. 11 shows the source current harmonic spectrum with a THD of about 42%. Thus the above simulated results show that the diode bridge rectifiers and phase-controlled converters create serious power quality problems in terms of distortion of the source current and deterioration of input power factor.
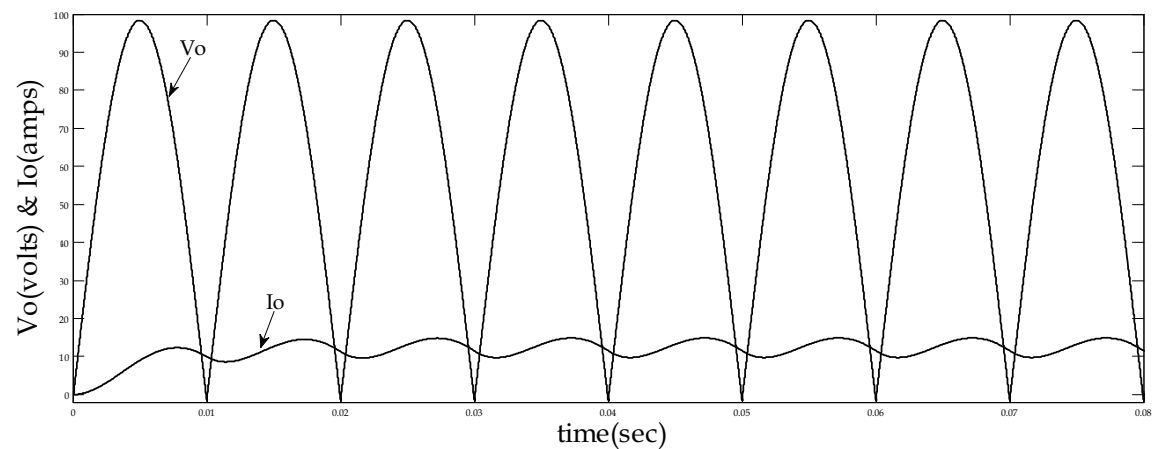

Fig. 3. Load voltage and load current waveforms of a single-phase bridge rectifier with R-L load
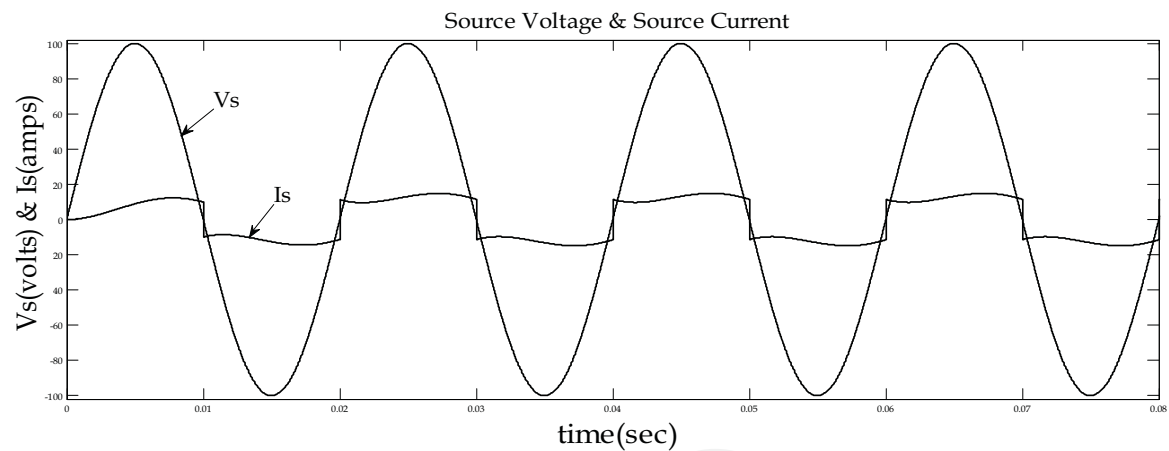

Fig. 4. Source voltage and source current waveforms of a single-phase bridge rectifier with R-L load
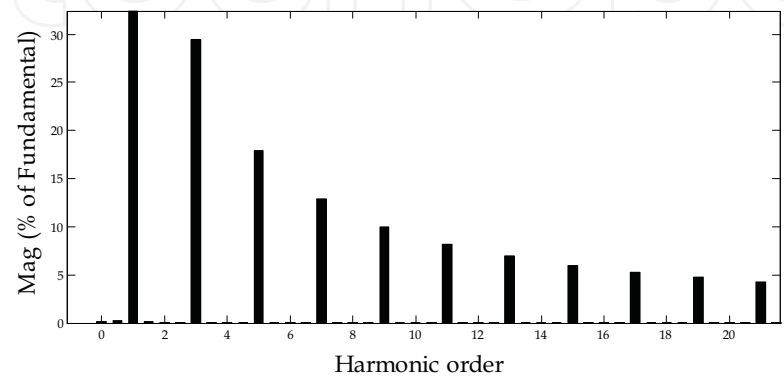

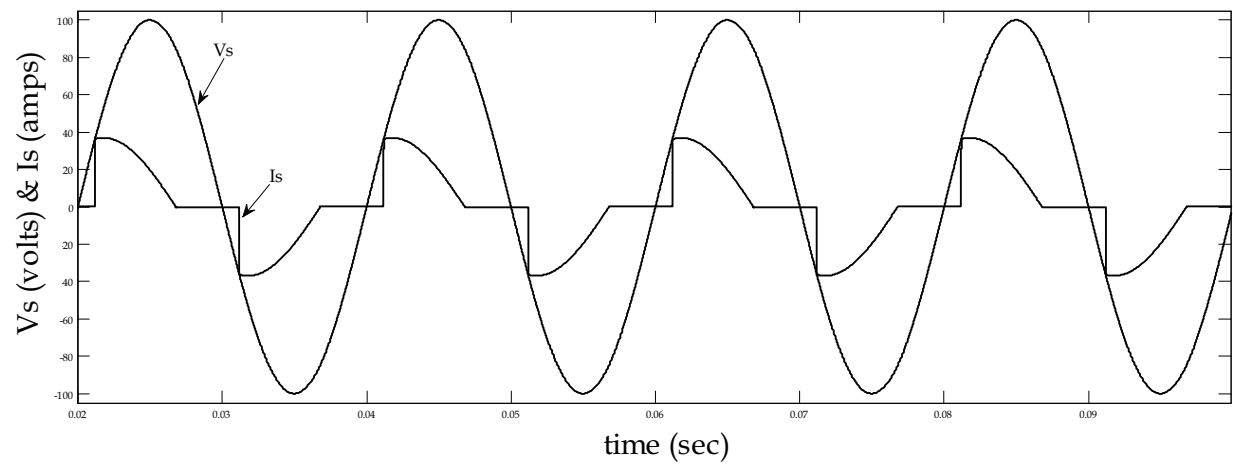Fig. 5. Harmonic spectrum of source current

Fig. 6. Source voltage and source current waveforms of a single-phase practical bridge rectifier
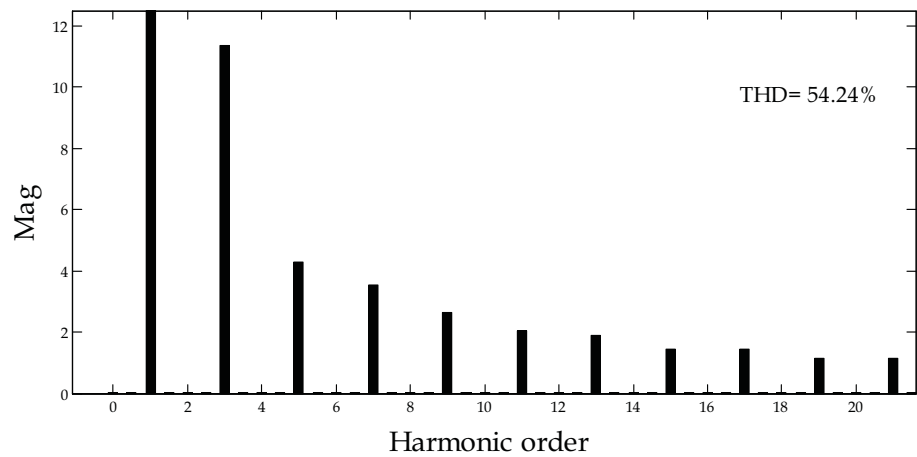

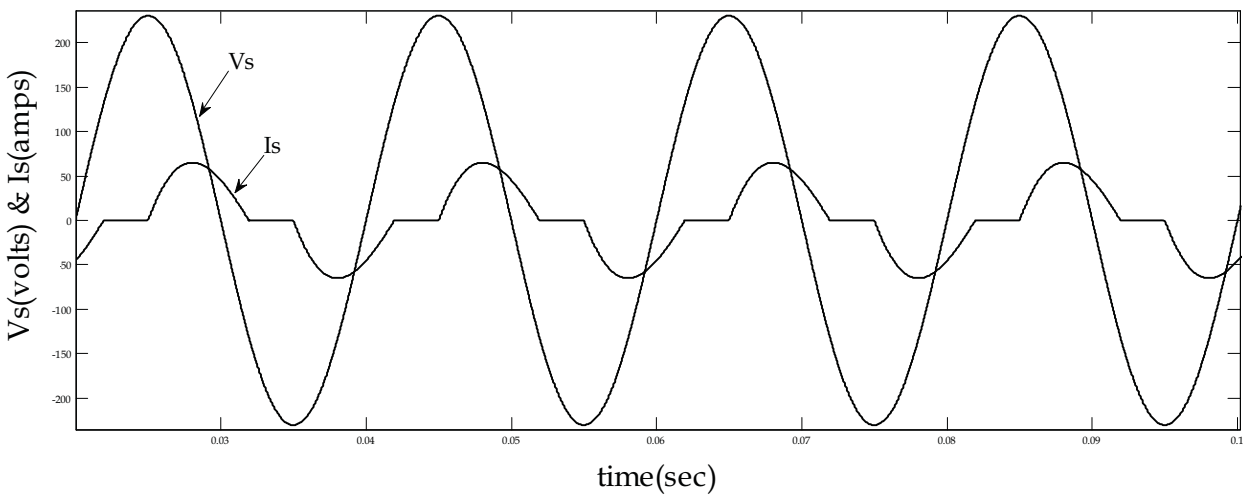Fig. 7. Harmonic spectrum of source current

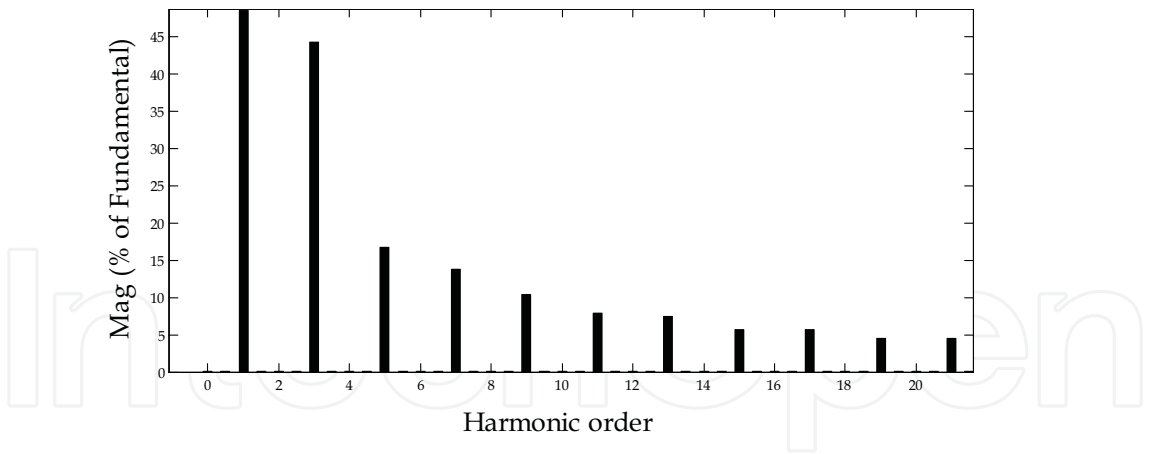Fig. 8. Source voltage and source current waveforms of a single-phase fully-controlled converter at α=90°

Fig. 9. Harmonic spectrum of source current
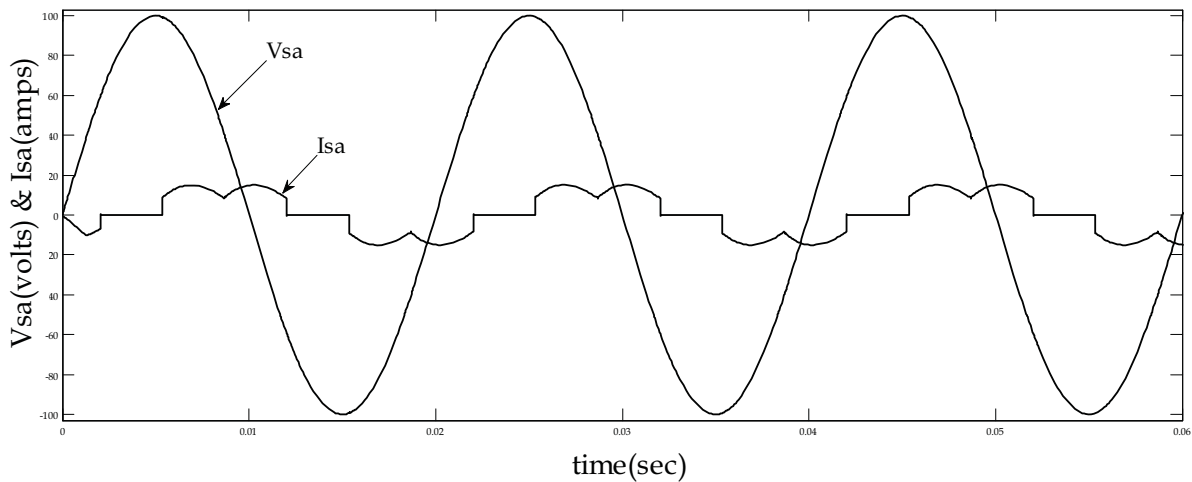

Fig. 10. Source voltage and source current waveforms of a three-phase line- commutated converter at α=90°
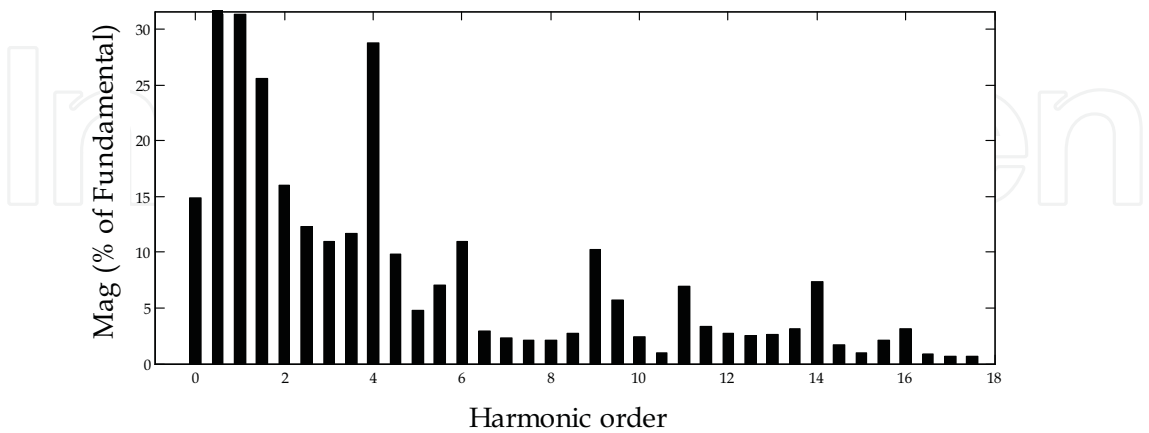

Fig. 11. Harmonic spectrum of source current

AC/DC power converters are extensively used in various applications like power supplies, DC motor drives, front-end converters in adjustable-speed AC drives, HVDC transmission, SMPS, fluorescent lights (with electronic ballasts), utility interface with non-conventional

energy sources, in process technology like welding, power supplies for telecommunications systems, aerospace, military environment and so on. Traditionally, AC-DC power conversion has been dominated by diode or phase-controlled rectifiers which act as non-linear loads on the power systems and draw input currents which are rich in harmonics and have poor supply power factor, thus creating the power quality problem for the power distribution network and for other electrical systems in the vicinity of rectifier. The other associated problems with these converters include:

- Large reactive power drawn by rectifiers from the power system which requires that the distribution equipment handle large power, thus increasing its volt-ampere ratings;
- Voltage drops at the buses;
- Higher input current harmonics resulting in the distorted line current which tends to distort the line voltage waveform. This often creates problems in the reliable operation of sensitive equipment operating on the same bus;
- Increased losses in the equipments (due to harmonics) such as transformers and motors connected to the utility;
- Electromagnetic interference with the nearby communications circuits;
- Excessive neutral current, resulting in overheated neutrals. The currents of triplen harmonics, especially odd harmonics (3rd, 9th, 15th,…) are actually additive in the neutral of three-phase Y-connected circuits;
- Incorrect reading meters, including induction disc-type W-hr meters and averaging type current meters;
- Blown-fuses on power factor correction capacitors due to high voltages and currents from resonance with line impedance and capacitor bank failures;
- Mal-operation of equipments such as computers, telephone systems, and electronic controllers;
- Nuisance operation of protective devices including false tripping of relays and failure of a UPS to transfer properly, especially if the controls incorporate zero-crossing sensing circuits;
- Damaging dielectric heating in cables and so on.

SCR=I/I$_1$	<II	II<h<17	17<h<23	23<h<35	35<h	TDD
<20	4.0	2.0	1.5	0.6	0.3	5.0
20-50	7.0	3.5	2.5	1.0	0.5	8.0
50-100	10.0	4.5	4.0	1.5	0.7	12.0
100-1000	12.0	5.5	5.0	2.0	1.0	15.0
>1000	15.0	7.0	6.0	2.5	1.4	20.0

Table 1. IEEE 519 Current Distortion Limits

Various standards are set to limit the harmonics by nonlinear loads. IEEE standard 519 was first issued in 1991. It gave the first guidelines for system harmonics limitations and was revised in 1992 [10]. IEEE 519-1992 Recommended Practices and Requirements for Harmonic Control in Electrical Power Systems provide the guidelines for determining what are the acceptable limits. The harmonic limits for current depend on the ratio of Short Circuit Current (SCC) at the Point of Common Coupling (PCC) to the average Load Current of maximum demand over one year, as illustrated in Table 1. Thus the basic philosophy of IEEE 519-1992 is to limit the harmonic current injected into the power system and to make

utility responsible for maintaining the voltage distortion. The IEC 61000 series is an internationally accepted set of standards and comprises of IEC 61000-3-2, 61000-3-3, 61000-3-4, 61000-3-5, and 61000-3-6. However, IEC 61000-3-4 is the most relevant one for industrial installations. The IEEE 519 standard limits the harmonics primarily at the service entrance, while IEC-3-2 is applied at the terminals of end-user equipment.

3. Classical solutions and recent trends

Classically, shunt passive filters consisting of tuned LC filters and/or high pass filters are used to suppress the harmonics and power capacitors are employed to improve the power factor of the utility/mains. The shunt passive filters are tuned most of the time to a particular harmonic frequency to be eliminated so that a low impedance is offered at the tuned frequency than the source impedance in order to reduce the harmonic current flowing into the source. Thus, the filtering characteristics are determined by the impedance ratio of the source and passive filter. Therefore the shunt passive filters suffer from the following drawbacks:

1. The source impedance, which is not accurately known and varies with the system configuration, strongly influences the filtering characteristics of the shunt passive filter.
2. The shunt passive filter acts as a sink to the harmonic current flowing from the source. In the worst case, the filter may fall in series resonance with the source impedance.
3. At a specific frequency, an anti-resonance or parallel resonance may occur between the source impedance and the shunt passive filter, which is also called the harmonic amplification.
4. As both the harmonics and the fundamental current component flow into the filter, the capacity of filter must be rated by taking into account both the currents.
5. Increase in harmonic current component can overload the filter.
6. If a good level of compensation is required, one needs as many filters as the number of harmonics to be eliminated

Conventional methods of var compensation are based on the vars generated or absorbed by the passive elements having energy storage capability. Dynamic compensation is achieved either by Switched Capacitor Var Compensators or Switched Capacitor and Thyristor Controlled Reactors. As the vars generated or absorbed are directly proportional to the energy storage capability of the passive elements used, their size increases with the increment in the vars to be compensated. Introduction of the sizeable inductors and capacitors into the system may lead to resonance created by the peripheral low frequency current sources. Moreover, the capability of this class of compensators to manipulate vars depends on the voltage level prevailing at the point where they are connected. Since the bus voltage reduces as the var demand increases, the compensators fail to perform when their participation is most needed. Also, they pollute the utility with low order harmonics which are difficult to filter. The sensitivity of these problems has attracted the attention of researchers to develop the techniques with adjustable and dynamic components. Extensive research is being carried out in the field of harmonics and reactive power compensation to overcome these limitations. With the continuous proliferation of nonlinear type loads, the requirements of power compensation involved avoidance of harmonic current generation also in addition to compensating for the reactive power generation. The equipments used for the harmonic compensation in addition to var compensation are known as Active Power Filters (APFs) [1,5,11,22]. These filters have provided the required harmonic filtering and

control performance in comparison to conventional shunt passive filters and static var compensators. The objectives of active filtering are to solve these problems by combining the advantages of regulated systems with reduced rating of the necessary passive components. The APFs are generally built around a PWM converter with capacitor/inductor on its DC side. The PWM converter switches are controlled to draw/supply a compensating current from/to the utility so that it cancels the current harmonics on the AC side by generating the nonlinearities opposite to the load nonlinearities and makes the source current almost sinusoidal which may be in phase or phase displaced with mains voltage, based on both harmonic and reactive power compensation requirements or only harmonics compensation requirement. In addition to the harmonics and reactive power compensation, APFs are also used to eliminate voltage harmonics, for load balancing, to regulate the terminal voltage, to suppress the voltage flickers, etc. These wide range of objectives are achieved either individually or in combination depending upon the requirements, control strategy and configuration, which is to be selected appropriately.

Based on the objectives, the APFs are broadly classified as Shunt Active Power Filter, Series Active Power Filter, and Hybrid Power Filter. However, the APFs suffer from the drawback of large size and rating (in some cases, the filter rating may be comparable with that of the load), complexity in the control and cost.

4. Improved power quality AC/DC converters

A new breed of AC/DC Power Converters has been developed to overcome all the drawbacks of passive filters, var compensators and active power filters used for harmonics and reactive power compensation. This new breed of converters is specifically known as Power Factor Correction Converters (PFCs), Switched Mode Rectifiers (SMRs), PWM Converters, Improved Power Quality Converters (IPQCs), and High Power Factor Converters (HPFCs). They are included as an inherent part of the AC-DC conversion system which produces excellent power quality at the line-side and load-side, higher efficiency, and reduced size. The power quality issues created by the use of conventional AC/DC converters are elegantly addressed by IPQCs. The output voltage is regulated even under the fluctuations of source voltage and sudden load changes. The PWM switching pattern controls the switchings of the power devices for input current waveshaping so that it becomes almost harmonic-pollution free and in phase with the source voltage, thus producing a nearly sinusoidal supply current at unity power factor without the need of any passive or active filter for harmonics and reactive power compensation. The reduced size of magnetics used in the converter system and the single-stage power conversion techniques have resulted in the development of reduced size, high power density, efficient, and reduced cost power converters. They have been made possible mainly because of the use of modern solid state, self-commutating power semiconducting devices such as Power MOSFETs, IGBTs, IGCTs, GTOs, etc. Remarkable progress in the capacity and switching speed of these devices has made it possible to develop the IPQCs for medium and large power applications. The parallel progress in the processors and high-speed DSPs has made it possible to implement the complex and computation-intensive control algorithms at very high speeds for the control of IPQCs. In fact, the development and progress in the fields of power semiconducting devices and DSPs has revolutionized the field of Power Electronics in recent past.

Improved Power Quality Converters are being developed with unidirectional and bidirectional power flow capabilities. Three-phase unidirectional IPQCs are realized using a

three-phase diode bridge followed by step-down chopper, step-up chopper, step-down/up chopper, isolated, forward, flyback, push-pull, half-bridge, full-bridge, SEPIC, Cuk, Zeta, and multilevel converters. A high-frequency isolation transformer offers reduced size, weight, cost, appropriate voltage matching and isolation. On the other hand, three-phase bidirectional IPQCs consist of basic converters such as push-pull, half-bridge, voltage source converter (VSC) topology, or current source converter (CSC) topology. Four-quadrant three-phase AC/DC power converters are normally implemented using matrix converters.

Due to all these advantages, IPQCs have generated tremendous interest among the researchers and application engineers to solve the increasing power quality problems. In fact, when an application engineer is at a decision stage, the active solution is advantageous over the passive filtering.

5. Converter topologies

Broadly, Three-phase Improved Power Quality Converters have been classified on the basis of the converter topology as Boost, Buck, Buck-Boost and Multilevel converters with unidirectional and bi-directional power flow and the type of converter used as unidirectional and bi-directional converters. B. Singh, et. al.   [23] presented the broad classification of three-phase IPQCs. In case of three-phase boost converters, the output voltage is greater than the peak input voltage. Unlike a single-phase boost converter, the voltage across the output capacitor does not have low-frequency ripple in balanced conditions. Thus a wide bandwidth voltage feedback loop can be used resulting in fast voltage control without distorting the input current references.

Fig. 12 shows one of the topologies of three-phase unidirectional boost converters [19]. High power-factor can be easily obtained when three-phase unidirectional boost converters are operated in discontinuous conduction mode (DCM) with constant duty cycles [28]. This is because the basic types of DC-DC converters, when operating in DCM, have self-power factor correction (PFC) property, that is, if these converters are connected to the rectified AC line, they have the capability to give higher power factor by the nature of their topologies. The peak of the supply-side inductor current is sampling the line-voltage automatically, giving boost converter the self-PFC property because no control loop is required from its input side. This is an advantage over continuous conduction mode (CCM) PFC circuit in which multi-loop control strategy is essential. However the input inductor operating in DCM cannot hold the excessive input energy because it must release all its stored energy before the end of each switching cycle. As a result, a bulky capacitor is used to balance the instantaneous power between the input and output. Also since the input current is normally a train of triangular pulses with nearly constant duty ratio, an input filter is necessary for smoothing the pulsating input current into a continuous one. Three-phase, unidirectional boost converters are widely used nowadays as a replacement of conventional diode rectifiers to provide unity input pf, reduced THD at AC mains and constant, regulated DC output voltage even under fluctuations of AC voltage and DC load.

Fig. 13 depicts one of the topologies of bidirectional boost converters. In case of bidirectional boost converters operating in CCM [9], since the input current is the inductor current, it can be easily programmed by current-mode control. Various current control techniques are available for controlling the input current so as to make the input current THD negligible associated with a unity input pf. We know that VSIs can reverse the power flow from load to DC link as a rectifier. However a standalone voltage source rectifier requires a special DC

bus able to keep voltage constant without the requirement of a voltage supply. This is accomplished with a DC capacitor and a feedback control loop. Boost converters operating in CCM give low dv/dt stress and hence produce low EMI emissions as compared to those operating in DCM. The softswitching techniques reduce the di/dt and dv/dt and hence improve the performance of bi-directional boost converters by causing low EMI emissions. The three-phase bi-directional boost PFCs are suitable for high power applications with improved performance as front-end converters with regeneration capability for variable-speed AC motor drives and also for hoists, cranes, lifts, BESS, line-interactive UPS, etc. [23]. Three-phase, buck converters produce output voltages less than the converter input voltage [8]. They have some attractive features compared to boost rectifiers such as meeting the requirement of varying controllable output DC voltage, inherent short-circuit protection, and easy inrush current. One of the topologies of three-phase unidirectional buck converters is shown in Fig. 14. Their input currents can be controlled in the open loop and much wider voltage loop bandwidth can be achieved. A unidirectional buck converter is a replacement of the thyristor semi-converter with improved power quality at AC mains and output DC bus.
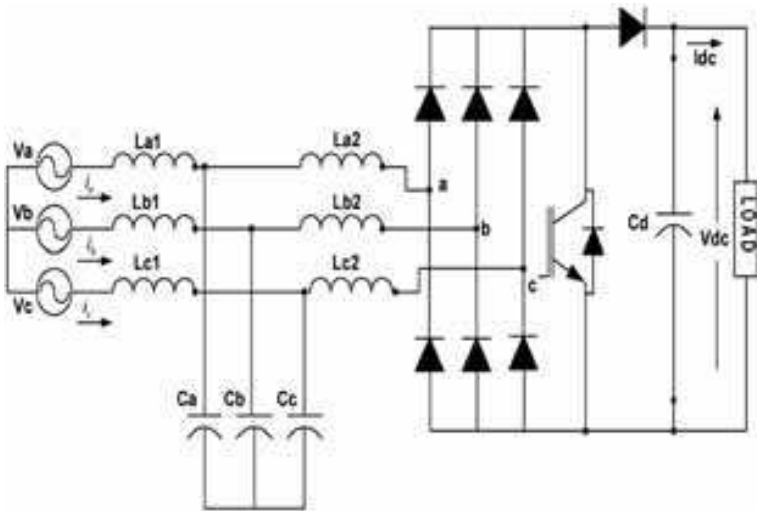

Fig. 12. Three-phase unidirectional boost converter
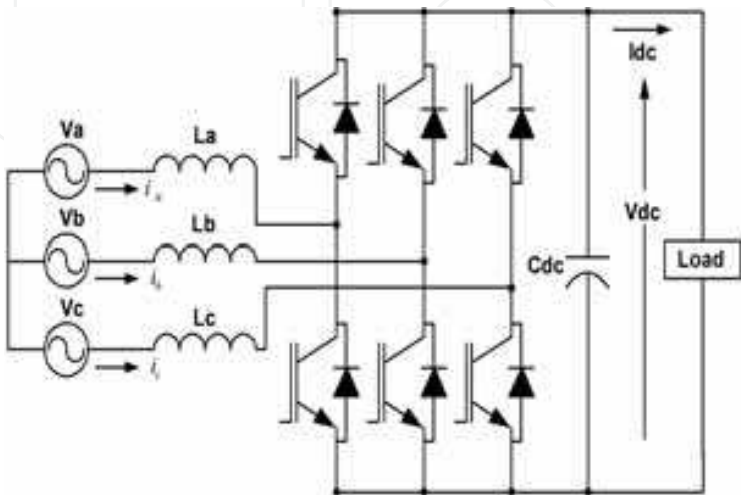

Fig. 13. VSI-bridge-based bidirectional boost converter
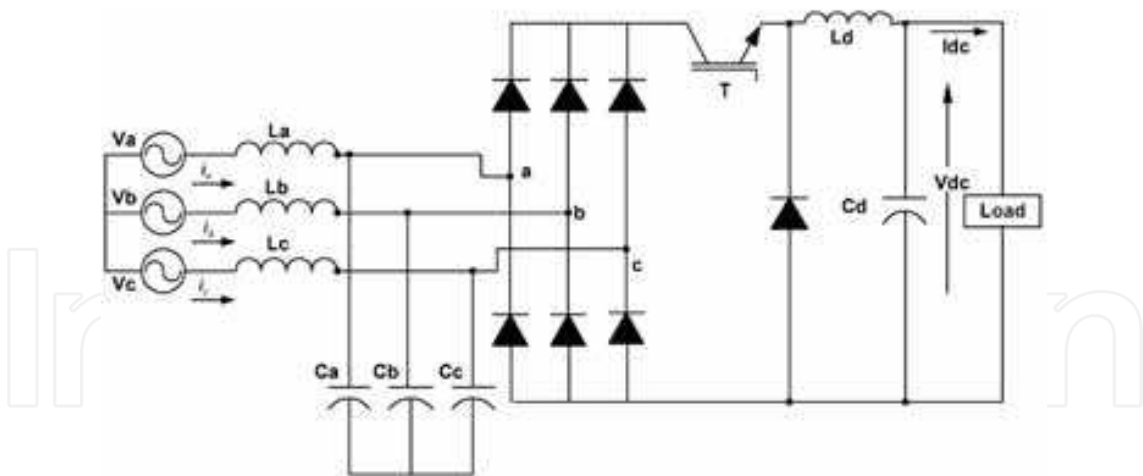
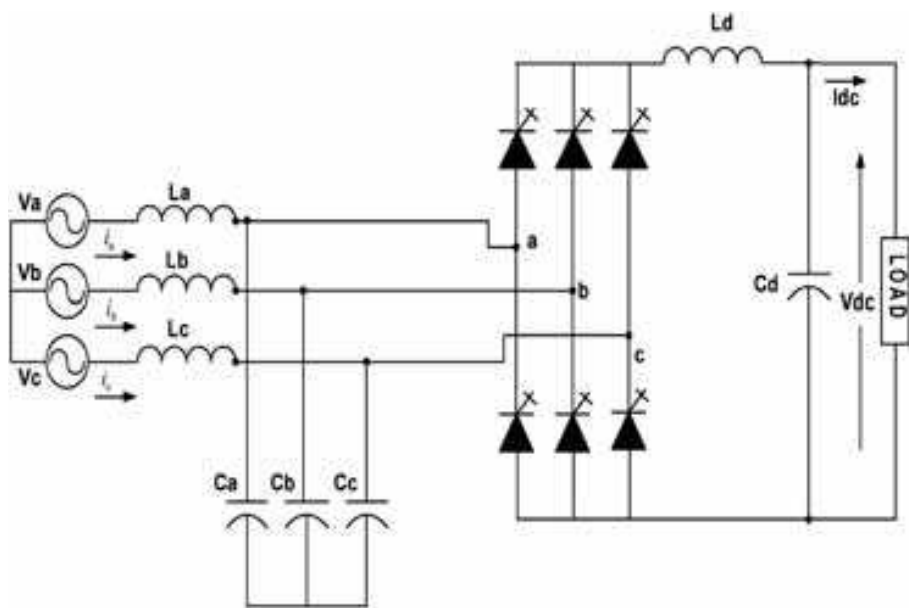Fig. 14. Single-switch unidirectional buck converter

Fig. 15. GTO-based bidirectional buck converter

Fig. 15 shows one of the topologies of the bidirectional buck converter [23]. A three-phase bidirectional buck converter provides a similar function as a conventional thyristor bridge converter but with improved power quality such as high power factor and reduced harmonic currents at AC mains and fast regulated output voltage with reversible power flow [6,14,27]. Two buck converters connected in anti-parallel provide the behaviour similar to a dual converter for four-quadrant operation with improved power quality and fast response.

In three-phase boost converters, the output voltages lower than the supply voltage cannot be achieved. Also in three-phase buck converters, the output voltages higher than the supply voltage cannot be achieved. However, it has the inherent DC short-circuit current and inrush current limitation capability. The three-phase buck-boost type AC/DC converters have step-up or step-down output voltage characteristics and also the capability of limiting the inrush and DC short-circuit currents. Therefore this type of converter is convenient for several power supplies and is highly suitable for input pf correction [7,12,13]. Fig. 16 depicts one of the topologies of three-phase unidirectional buck-boost converters.

There are some applications which require output DC voltage widely varying from low voltage to high voltage with bidirectional DC current as four-quadrant operation and bidirectional power flow. As discussed by B. Singh, et. al. [23], the simplest way of realizing a three-phase bidirectional buck-boost converter is by using a matrix converter as shown in Fig. 17. The three-phase bidirectional buck-boost converters can be used for medium power applications in telecommunications and also for motor drive control.
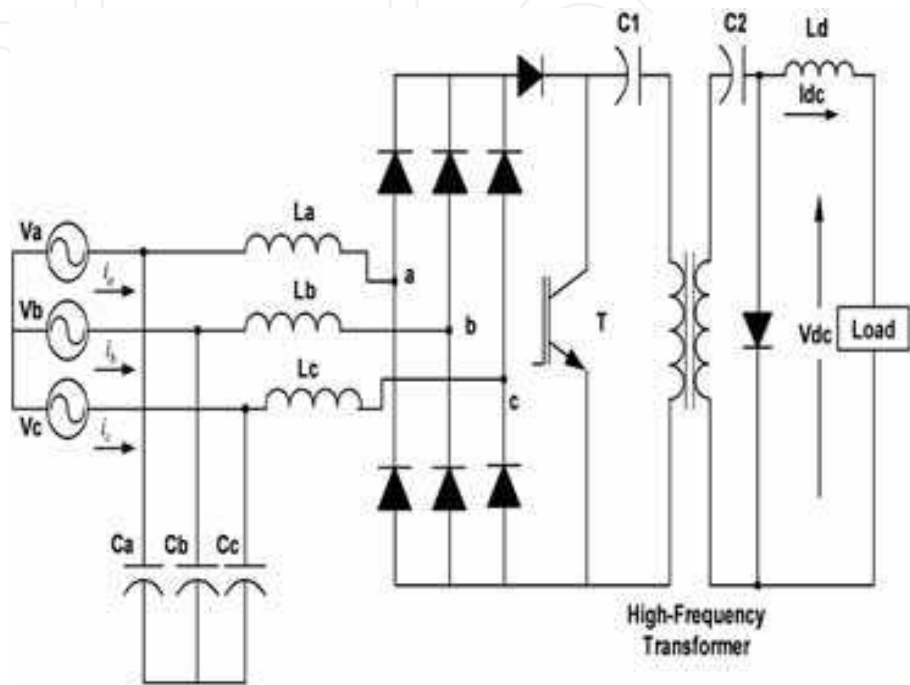
Fig. 16. Isolated cuk-derived unidirectional buck-boost converter
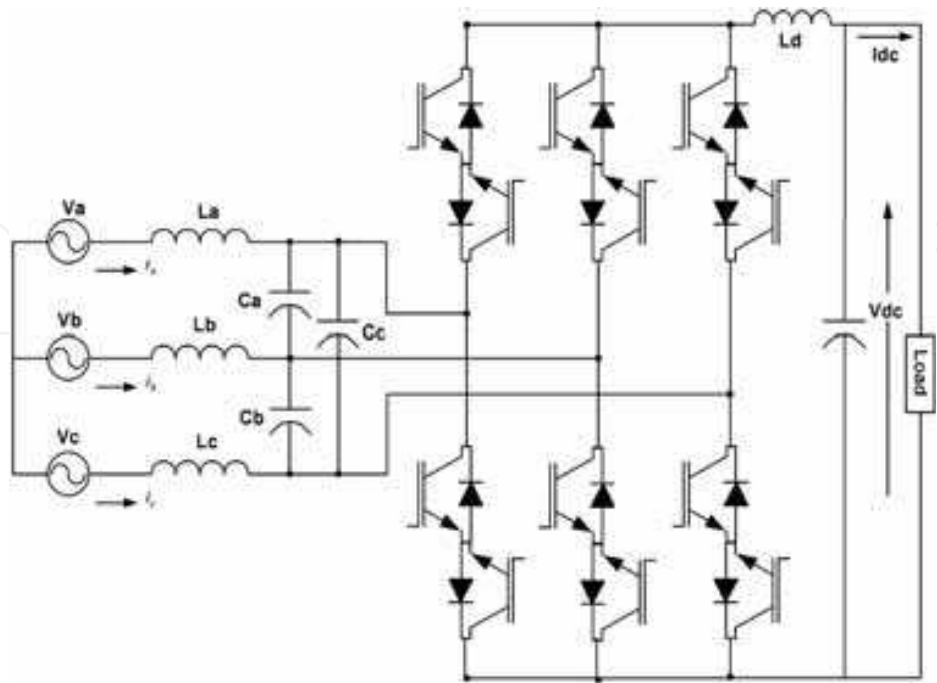
Fig. 17. Matrix-converter-based bidirectional buck-boost converter

Multilevel Converters (MLCs) are gaining widespread popularity because of their excellent performance with reduced THD of input current, high supply power factor, ripple-free regulated DC output voltage, reduced voltage stress of devices, reduced dv/dt stresses, and hence lower EMI emissions [3,15,16,17,18,20,21,24,25]. They also avoid the use of transformers in some applications which further enhances the efficiency of these converters. The sinusoidal source currents at unity power factor are produced at reduced switching frequencies in comparison with their two-level counterparts. Moreover since an MLC itself consists of series connection of switching power devices and each device is clamped to the DC-link capacitor voltage through the clamping diodes, it does not require special consideration to balance the voltages of power devices.

On the other hand, the series connection of power devices is a big issue in two-level converters. Moreover, in case of a multilevel converter, each device is stressed to a voltage $V_{dc}/(n-1)$, where V_{dc} is the DC-bus voltage and n is the number of levels. Hence the device stress is considerably reduced as the number of levels increases [15]. This makes multilevel converters the best choice for the high-voltage and high-power applications and they have invited a lot of attention for high-power industrial applications. Nevertheless, the neutral point of the neutral point clamped converter is prone to fluctuations due to irregular charging and discharging of the output capacitors [20]. Thus the terminal voltage applied at the switches on DC side can exceed that imposed by the manufacturer. Moreover the device count is large in multilevel converters and complex control is involved [15].

Fig. 18 depicts one of the topologies of three-phase, unidirectional multi-level converters [23]. These converters also offer boost operation for the output voltage with unidirectional power flow.
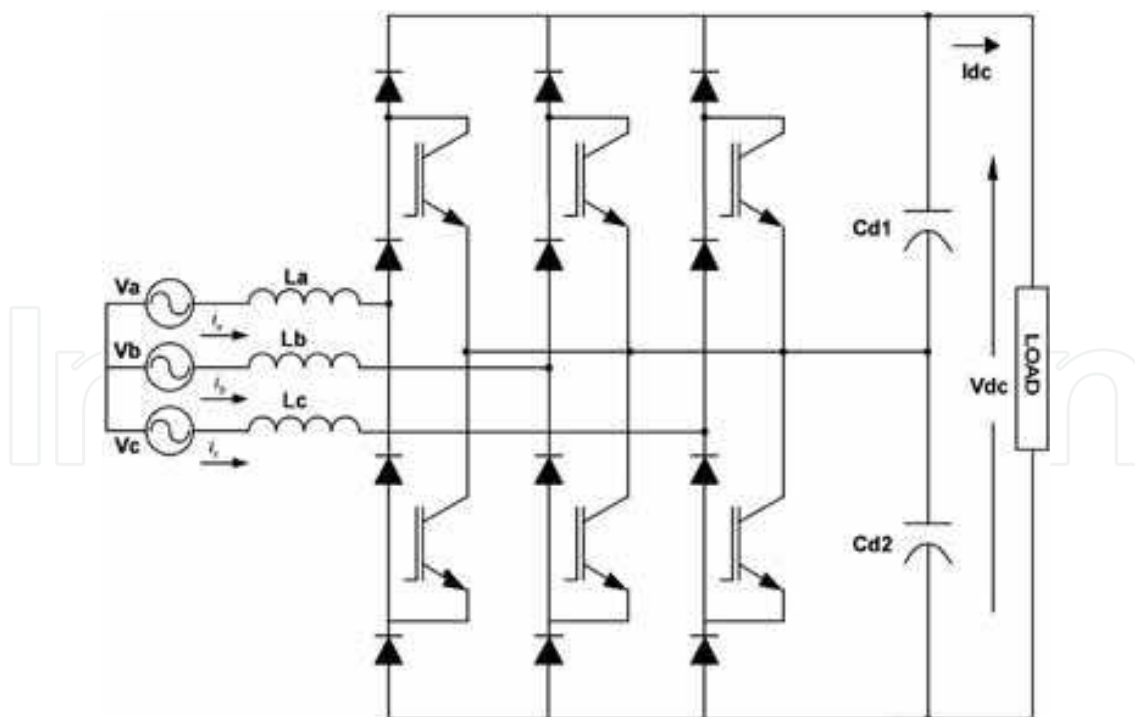

Fig. 18. Six-switch unidirectional three-level converter

J. S. Lai and F. Z. Peng [15] classified the bidirectional MLCs into three main categories as diode-clamped MLC, flying capacitor MLC, and cascaded MLC as shown in Fig. 19. In
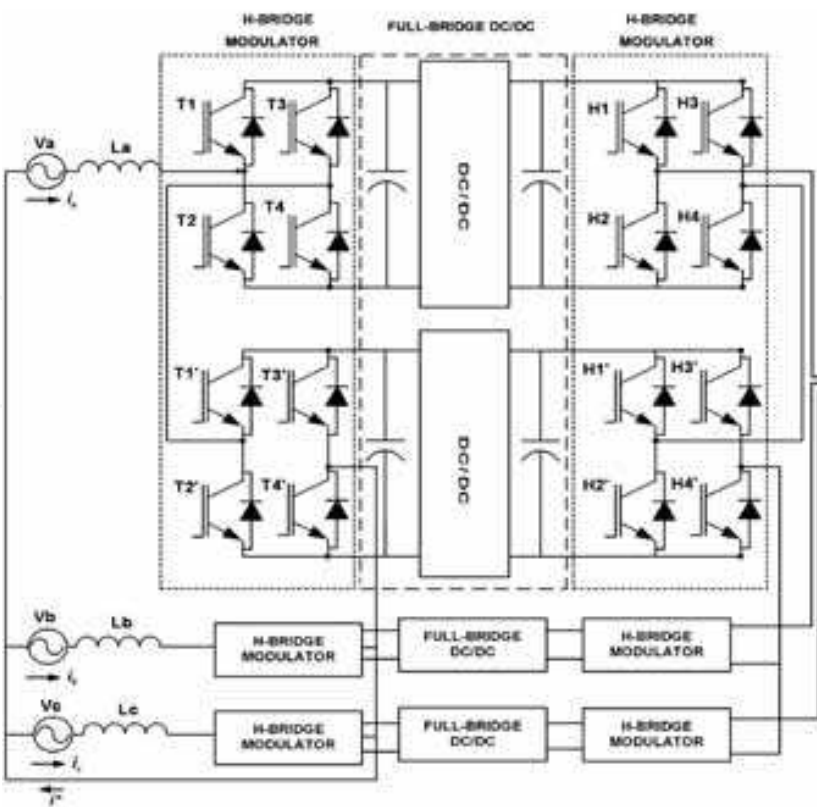
fact, all the three types of multilevel bidirectional converters shown in this Figure can be used in reactive power compensation without having voltage unbalance problem.
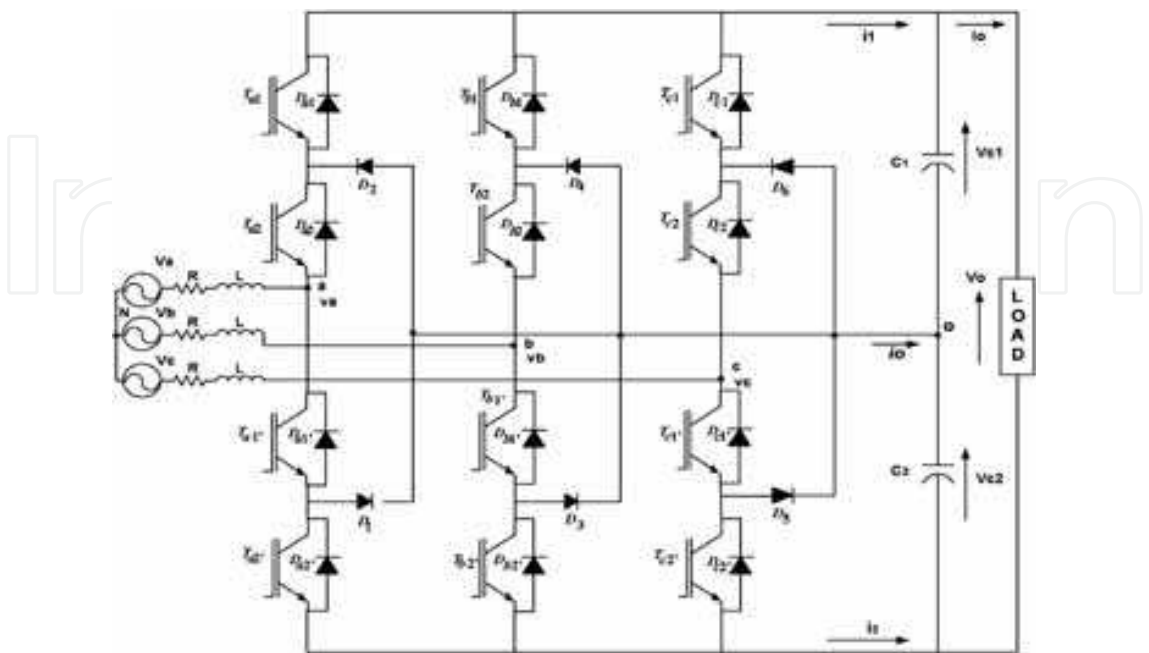
(a)
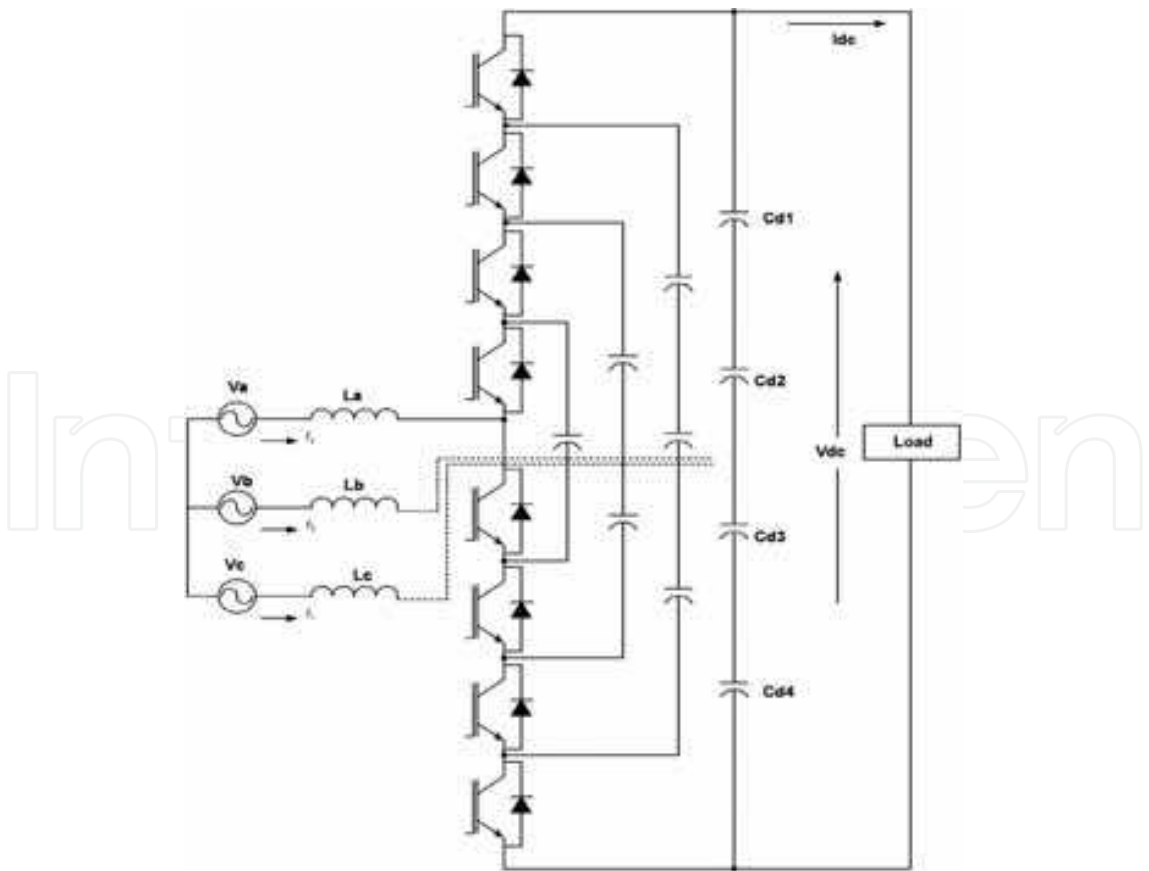
(b)

(c)

Fig. 19. (a) Three-level diode-clamped bidirectional converter (b) Five-level flying capacitor bidirectional converter (c) Three-level converter using H-bridge (cascade) modules

In case of diode-clamped multilevel converters, the reactive power flow control is easier. But the main drawback of this converter is that excessive clamping diodes are required when the number of levels is high. In case of flying capacitor multilevel converters, large amount of storage capacitors provides extra ride through capabilities during power outage. But the main drawback is that a large number of capacitors is required when the number of levels is high which makes the system less reliable and bulky and thus more difficult to package. In case of cascaded multilevel converters, least number of components is required and modularized circuit layout and packaging is possible because each level has the same structure and there are no extra clamping diodes or voltage balancing capacitors. But the main drawback is that it needs separate DC sources, thus making its applications somewhat limited. A comparison of different types of three-phase MLCs, in terms of power components required in each type of converter has been given in a tabular form in Table 2.

Converter Type	Device Count		
	Diode-Clamped MLC	Flying-Capacitor MLC	Cascaded MLC
Main Power Switches	$(n-1)\times 2$	$(n-1)\times 2$	$(n-1)\times 2$
Clamping Diodes	$(n-1)\times(n-2)$	0	0
DC-Bus Capacitors	$(n-1)$	$(n-1)$	$(n-1)/2$
Balancing Capacitors	0	$(n-1)\times(n-2)/2$	0

Table 2. Comparison of different types of Multilevel Converters

In this table, *n* specifies the number of levels. Multilevel bidirectional converters are used at high power ratings at high voltages with boost voltage for bidirectional power flow. Since the multilevel rectifiers offer a number of advantages over their two-level counterparts and are a promising alternative to medium and high voltage and high power industrial applications, they are a subject of intense research these days.

6. Three-phase neutral-point clamped bidirectional rectifier

Improved Power Quality Converters are now seen as a viable alternative over the conventional methods of improving the power quality. This new breed of AC/DC converters gives excellent power quality indices like nearly unity input power factor, negligible THD in source current, reduced ripple factor of load voltage and fast-regulated load voltage. Among the various topologies of improved power quality converters developed so far, multi-level converters provide the viable solution for medium to high power industrial applications at high voltages and have recently developed a great interest among the researchers. Diode-clamped multilevel converter is the most popularly used topology among the multilevel power converters [15,17,21,24,26].

Various modulation strategies have been researched for the control of multilevel bidirectional converters. Among the various modulation strategies, space vector PWM (SVPWM) has been found the best for the control of these converters as this modulation technique results in lower switching frequency, better utilization of DC-bus voltage, negligible input current THD and addresses the issue of DC-bus capacitor voltage unbalance in the neutral-point clamped converters. In fact, the large number of redundant switching states in SVPWM is being exploited for the balance of DC-bus capacitor voltages. The development of high speed DSPs has made possible the implementation of computation-intensive algorithm like SVPWM in multilevel converters where the complexity and computational burden increases excessively, especially for higher number of levels. The development of DSPs for real-time simulation has added a new dimension in the easy implementation of very complex control algorithms for the control of multilevel converters.

The performance of a three-phase, three-level bidirectional rectifier using sinusoidal pulse-width modulation (SPWM) technique and space vector pulse-width modulation (SVPWM) technique is evaluated in this chapter. A comparative evaluation of the three-level converter using above modulation techniques is performed to emphasize the advantages offered by SVPWM technique over SPWM technique for the control of these converters.

Fig. 20 shows the power circuit of a three-phase three-level (neutral-point clamped) bidirectional rectifier. In this circuit topology, each power switch is stressed to half the DC bus voltage instead of full DC bus voltage as is the case with two-level converters.

The independent power switches (T_{x1} and T_{x2}, $x = a, b, c$) are controlled in each leg of the converter. The constraints for four power switches in an arm of the converter are defined so as to avoid the power switches conducting at the same time.

$$T_{xi} + T_{xi'} = 1 \tag{1}$$

where $T_{xi} = 1$(or 0) if the power switch T_{xi} is turned on (or off) and $x = a,b,c$ and $i = 1,2$.

Four switching states are possible for each rectifier leg. However, only three valid switching states can be generated to achieve three voltage levels on the AC terminals of rectifier leg. The equivalent switching functions of the rectifier are defined below:

$$S_a = \begin{cases} 1 & if \ T_{a1} \ and \ T_{a2} \ are \ turned \ on \\ 0 & if \ T_{a1'} \ and \ T_{a2} \ are \ turned \ on \\ -1 & if \ T_{a1'} \ and \ T_{a2'} \ are \ turned \ on \end{cases} \tag{2}$$

$$S_b = \begin{cases} 1 & if \ T_{b1} \ and \ T_{b2} \ are \ turned \ on \\ 0 & if \ T_{b1'} \ and \ T_{b2} \ are \ turned \ on \\ -1 & if \ T_{b1'} \ and \ T_{b2'} \ are \ turned \ on \end{cases} \tag{3}$$

$$S_c = \begin{cases} 1 & if \ T_{c1} \ and \ T_{c2} \ are \ turned \ on \\ 0 & if \ T_{c1'} \ and \ T_{c2} \ are \ turned \ on \\ -1 & if \ T_{c1'} \ and \ T_{c2'} \ are \ turned \ on \end{cases} \tag{4}$$

Three valid operation modes in leg-*A* of the converter are as:

Operation mode 1 (S_a = 1): In this mode, the power switches T_{a1} and T_{a2} are turned on. The AC terminal voltage $v_a{'}$ (or v_{ao}) is equal to $V_o/2$ (assuming $V_{c1} = V_{c2}$). In this case, the boost inductor voltage $v_L = v_a - V_o/2 < 0$ if the voltage drop across the equivalent series resistance is neglected. Therefore, the line-current i_a decreases and the current slope is $(v_a - V_o/2)/L$.

The line-current i_a will charge or discharge the DC-bus capacitor C_1 if the AC system voltage V_a is positive or negative, respectively.

Operation mode 2 (S_a = 0): In this mode, the power switches $T_{a1}{'}$ and T_{a2} are turned on and the AC terminal voltage v_{ao} is equal to zero. The boost inductor voltage $v_L = v_a$. The line-current increases or decreases during the positive or negative half cycle of mains voltage v_a, respectively. The converter input current i_a will not charge or discharge any one of the DC bus capacitors in this mode of operation. In fact, the input power is stored in the boost inductor during this mode.

Operation mode 3 (S_a = -1): In this mode, the power switches $T_{a1}{'}$ and $T_{a2}{'}$ are turned on and a voltage level of $-v_o/2$ is generated on the AC terminal voltage v_{ao}. The boost inductor voltage $v_L = v_a + V_o/2 > 0$ and the line current increases. The current slope is $(v_a + V_o/2)/L$. The line current i_a will charge or discharge the DC bus capacitor C_2 during the positive or negative half of mains voltage v_a, respectively. The operation modes are similar in converter legs *B* and *C* to control the line currents i_b and i_c.

Table 3 shows the valid switching states of the power switches of three legs and the corresponding voltages on the ac side of the rectifier.

s	T_{x1}	T_{x2}	$T_{x1'}$	$T_{x2'}$	v_{xn}
1	1	1	0	0	$V_1 = V_o/2$
0	0	1	1	0	0
-1	0	0	1	1	$V_2 = -V_o/2$

x = a, b, c.

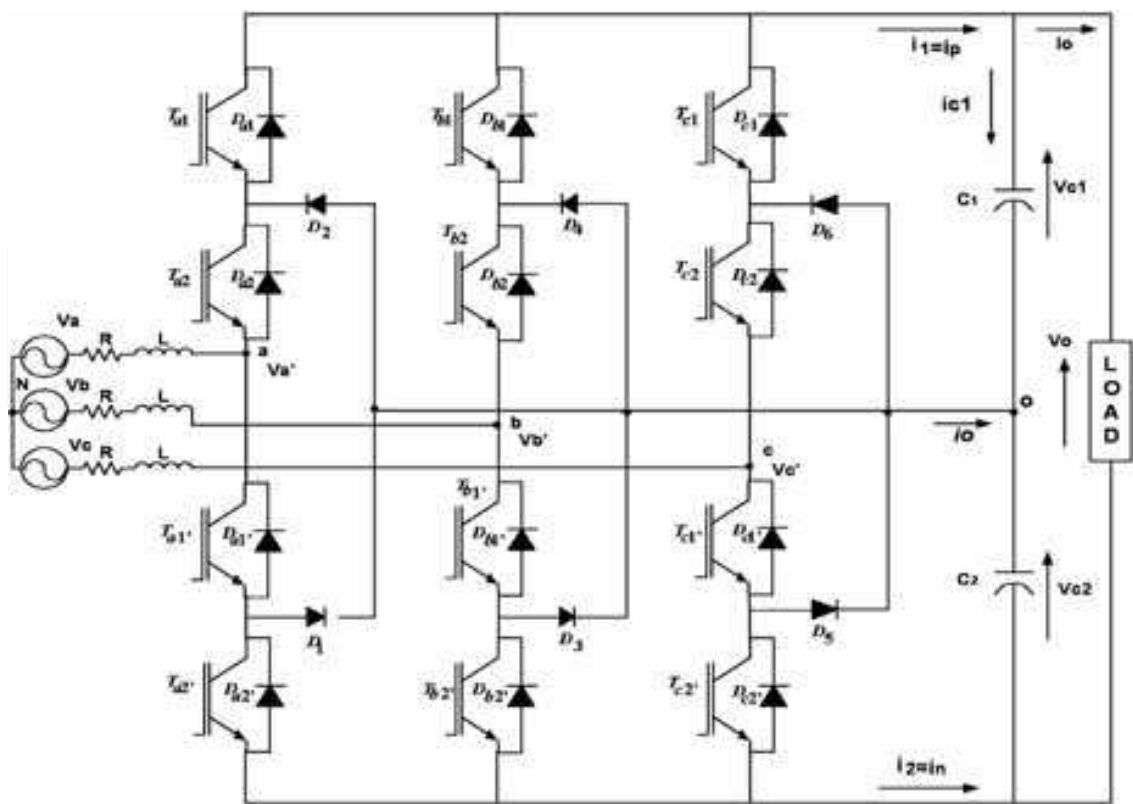Table 3. Valid switching states and corresponding voltages

Fig. 20. Three-level diode-clamped bidirectional rectifier

7. Sinusoidal pulse width modulation (SPWM)

In this technique, the neutral point of DC bus is connected to the neutral of three-phase AC source as shown in Fig. 21. Three unipolar PWM waveforms are generated on the three phases on input side of the converter based on carrier-based PWM scheme.

The equivalent switching function of the rectifier is defined as:

$$
s = \begin{cases} 1 & if \quad T_{x1} = T_{x2} = 1 \\ 0 & if \quad T_{x1'} = T_{x2} = 1 \\ -1 & if \quad T_{x1'} = T_{x2'} = 1 \end{cases} \tag{5}
$$

The supply side line-to-neutral voltage of the rectifier can be expressed as,

$$
v_{xo} = \frac{s(s+1)}{2} V_{c1} - \frac{s(s-1)}{2} V_{c2} =
$$
$$
= \frac{s^2}{2} \Delta V + \frac{s}{2} V_0 \tag{6}
$$

If the two capacitor voltages V_{c1} and V_{c2} are equal, i.e., $\Delta V=0$, then there are three voltage levels, $V_d/2$, 0 and $- V_d/2$, on the AC side (line-to-neutral voltages) of the rectifier. By proper combinations of the power switches of any arm, three different voltage levels are generated in the line-to-neutral voltage by the rectifier. The three valid modes for phase-leg A of the rectifier are described schematically in Fig. 22.
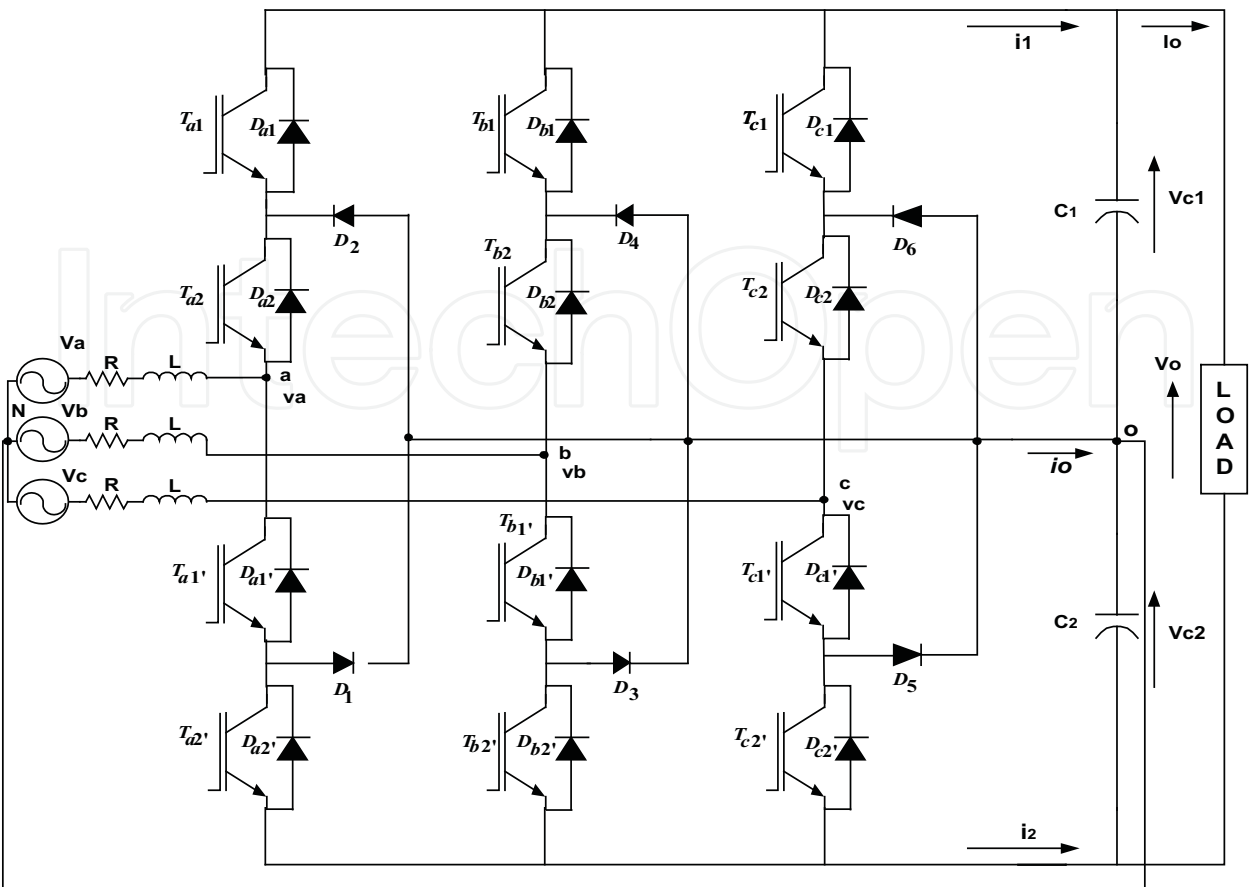
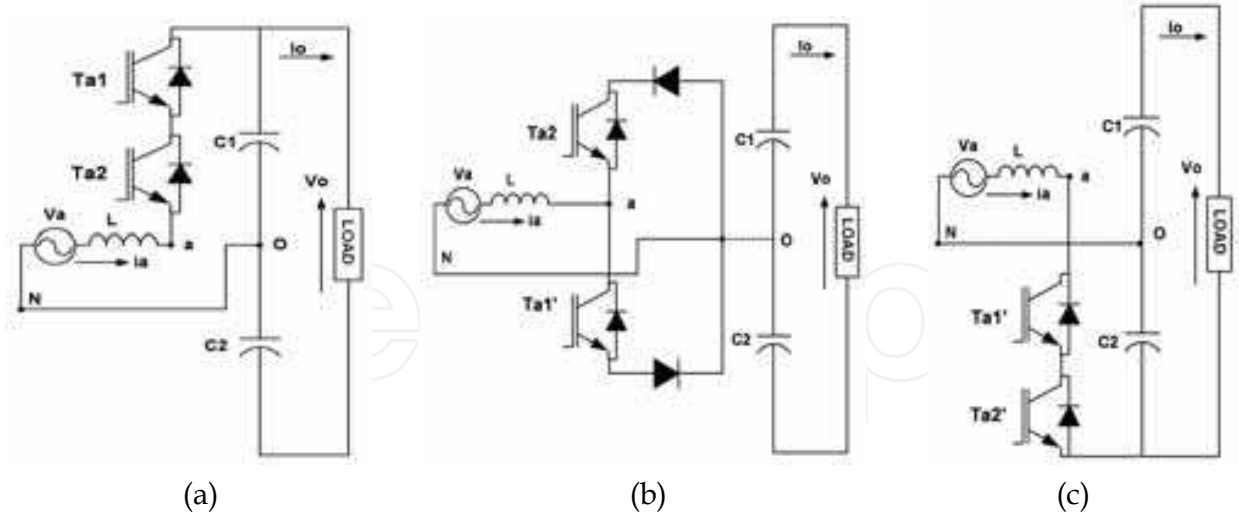Fig. 21. Adopted Three-Phase Neutral-Point Clamped Converter for SPWM Technique

(a)   (b)   (c)

Fig. 22. Three valid operating modes for phase *A* of NPC rectifier (a) Mode 1 ($v_{ao} = V_o/2$) (b) Mode 2 ($v_{ao} = 0$) (c) Mode 3 ($v_{ao} = -V_o/2$)

In the same manner, during the negative half cycle of mains voltage of phase *A*, two voltage levels, *0* and $-V_o/2$, are produced in v_{ao}. In this case, the switch $T_{a1'}$ is turned on and the switches T_{a2} and $T_{a2'}$ are turned on to achieve $v_{ao} = 0$ and $-V_o/2$ ($-V_{c2}$) respectively.

The sinusoidal PWM controller block and the generation of gating pulses is shown in Fig. 23.

(a)

(b)
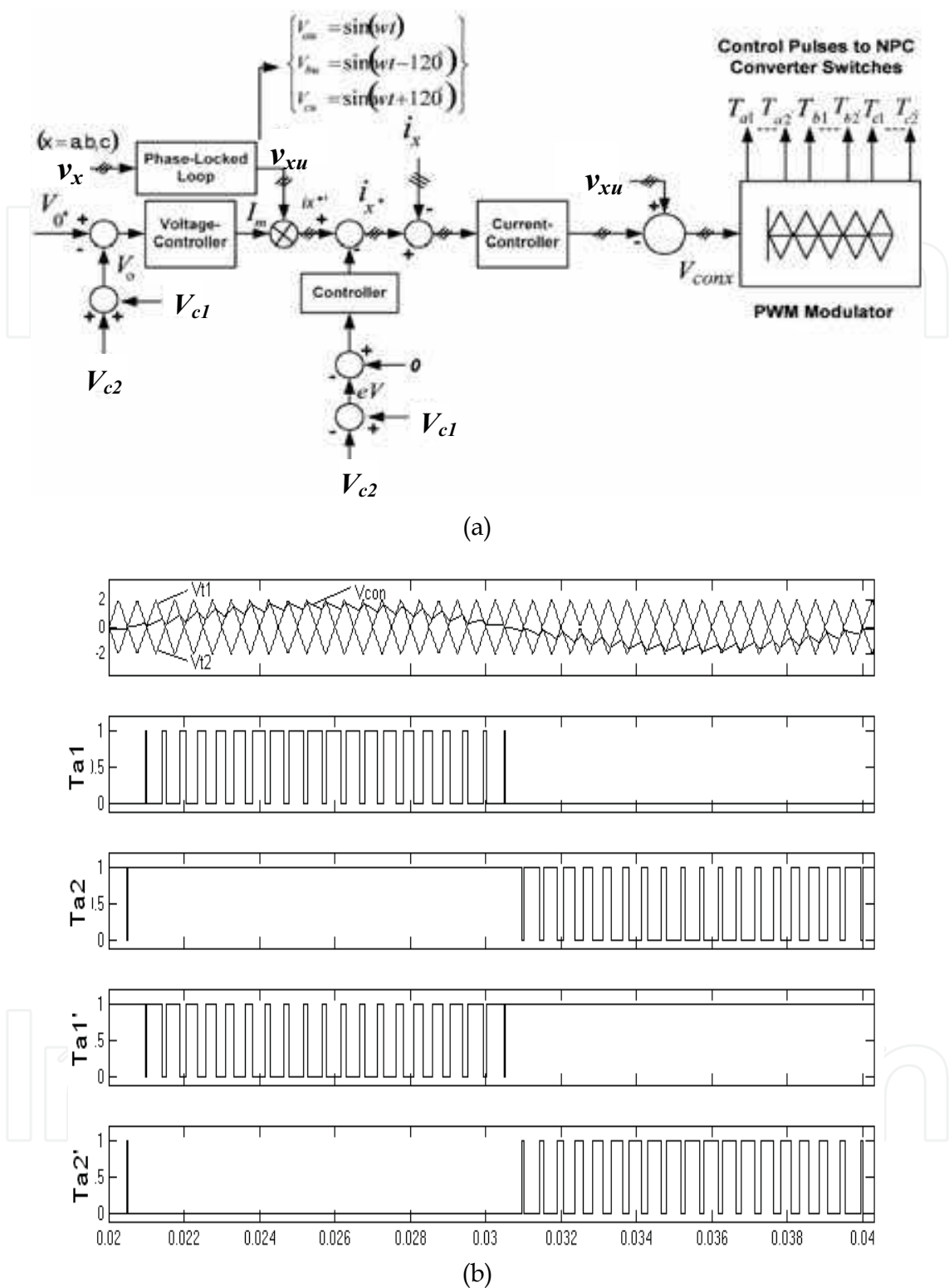
Fig. 23. (a) Block diagram of the PWM controller (b) Carrier-based PWM scheme (Control Pulses)

To regulate the DC bus voltage, a voltage controller is used to maintain the voltage at the desired reference value. The output of the voltage controller is multiplied by unit three-phase sinusoidal waveforms in phase with the mains three-phase voltages (obtained from a phase locked loop) to form three line-current commands for three phases of the rectifier. To

compensate the voltage unbalance between two capacitors in the DC link, a voltage compensator is added to the line-current commands. The line-current error between the current commands $i_{sx}{}^*$ and actual line current i_{sx} of each phase is fed to the current controller of that phase based on sine-triangle PWM scheme to track the line-current commands. The neutral point voltage on the DC link is controlled by power switches by adjusting the neutral point current i_0. By appropriate control, unipolar PWM voltage waveforms are generated on the three line-to-neutral voltages v_{ao}, v_{bo} and v_{co}.

Apply Kirchhoff's voltage law (KVL) on phase a (AC side) of the rectifier, we have

$$v_a = Ri_a + L\frac{di_a}{dt} + v_{ao} \tag{7}$$

From (6), for phase a (x = a),

$$v_{ao} = \frac{s^2}{2}\Delta V + \frac{s}{2}V_0 \tag{8}$$

According to (7), we have

$$v_a = Ri_a + L\frac{di_a}{dt} + \frac{s}{2}V_0 + \frac{s^2}{2}\Delta V \tag{9}$$

If the dc-link capacitor voltages are equal, equation (9) can be written as,

$$v_a = Ri_a + L\frac{di_a}{dt} + \frac{s}{2}V_0 \tag{10}$$

Assuming the ideal power switches, no power loss occurs in the converter and the instantaneous power at the input and output of converter are equal.

To obtain a general control law for the neutral point current, the DC side quantities can be given as,

$$i_1 = C\frac{dV_{c1}}{dt} + \frac{V_{c1} + V_{c2}}{R} \tag{11}$$

$$i_2 = -C\frac{dV_{c2}}{dt} - \frac{V_{c1} + V_{c2}}{R} \tag{12}$$

Neutral point current i_o is given by,

$$i_0 = -i_1 - i_2$$

$$i_o = -C\frac{d(V_{c1} - V_{c2})}{dt} \tag{13}$$

This equation yields,

$$\Delta V = (V_{c1} - V_{c2}) = -\frac{1}{C}\int i_o dt + constant \tag{14}$$

This signifies that a DC component in the neutral current i_o can be used to compensate the voltage unbalance on the dc side of converter (neutral point voltage). The adopted controller

for the rectifier as shown in Fig. 23(a) is supposed to fulfill all the control objectives. A proportional-integral (PI) voltage controller is employed in the outer loop control to maintain the DC-link voltage at the desired reference value. The line-current command is derived from the output of PI controller and the phase-locked loop (PLL) circuit and it is given by,

$$i_{x*'} = \left(k_p \Delta V_0 + k_i \int \Delta V_0 dt\right) \sin\left(\omega t + \theta\right) \qquad (15)$$

where

$$\begin{cases} \theta = 0° & for \quad phase \quad a \\ \theta = -120° & for \quad phase \quad b \\ \theta = 120° & for \quad phase \quad c \end{cases}$$

and $x = a,b,c$.

A three-phase PLL is used to generate three unit sinusoidal waves in phase with their corresponding supply voltages. To balance the neutral point voltage, the output of capacitor voltage balance controller is added to the line-current commands. The sensed line currents are compared with the respective reference line currents and the current errors thus generated are fed to the current controllers to track the source current commands. The carrier-based sinusoidal PWM scheme is employed for generating proper switching signals. Neglecting the high-frequency switching terms, we can write

$$v_{sx} = L.\frac{di_x}{dt} + V_{conx} \qquad (16)$$

where V_{conx} (x=a,b,c) is the modulating control signal of PWM converter derived from the closed-loop control scheme of the system.

From the control and gating signals as shown in Fig. 23(b), the switching signals of the power devices can be defined as,

$$s = \begin{cases} 1 & if \quad V_{conx} \rangle V_{t1} \\ 0 & if \quad V_{t1} \rangle V_{conx} \rangle V_{t2} \\ -1 & if \quad V_{t2} \rangle V_{conx} \end{cases} \qquad (17)$$

Hence,

$$T_{x1} = \frac{s(s+1)}{2} \qquad (18)$$

$$T_{x1'} = 1 - T_{x1} \qquad (19)$$

$$T_{x2'} = \frac{s(s-1)}{2} \qquad (20)$$

$$T_{x2} = 1 - T_{x2'} \qquad (21)$$

For a particular phase, in the positive half of the control signal V_{conx}, the power switch T_{x2} is turned on and the line current is controlled by turning on or off the power switch T_{x1}. In the negative half of V_{conx}, T_{x1} is turned off and turning on or off T_{x2} can control the line current to

follow the current command. For equal capacitor voltages ($V_{c1} = V_{c2} = V_0/2$), three voltage levels ($V_0/2$, 0, and - $V_0/2$) are generated on the AC side of the rectifier phase voltage $V_{xo'}$.

8. Performance evaluation

The performance of the NPC converter using SPWM technique is evaluated under ideal mains conditions and various performance indices are obtained after exhaustive simulations. MATLAB/Simulink and SimPowerSystems software has been used for simulation purposes. The system parameters chosen for simulations are given in the following Table 4.

System Parameters	
Supply-side parameters	**Load-side parameters**
Supply voltage: 110 volts (rms), 50 Hz	Load: R_o = 15 Ω, L_o = 5 mH
Boost Inductor: L = 4.5 mH, R = 0.4 Ω	DC-Bus capacitors: $C_1 = C_2$ = 4700 μF
Reference DC voltage: V_o^* = 400 volts	
Sampling frequency, f_s = 5 kHz	

Table 4. System parameters for Simulation

Fig. 24 shows the phase *A* source voltage and line-current waveforms for the rectification mode of operation. It is observed from this figure that the rectifier draws a sinusoidal current from the source at nearly unity power factor. Fig. 25 shows the frequency spectrum of line-current drawn by the rectifier. The line-current THD is 3.2%. Fig. 26 shows the source voltage and line-current waveforms when the converter is operated in inversion mode.
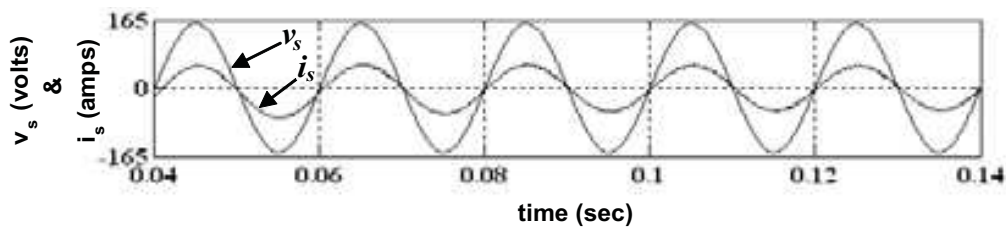

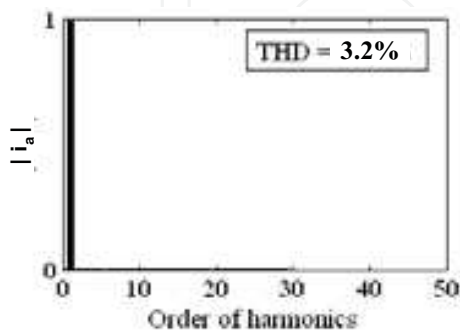Fig. 24. Phase *A* voltage and line-current waveforms for rectification mode of operation

Fig. 25. Frequency spectrum of phase *A* current

The line current is still sinusoidal in nature with very low THD. Fig. 27 shows the load voltage waveform. It is observed that the load voltage is regulated at the desired reference value of 400 volts with a smaller ripple factor of only 0.7 volt. Fig. 28 shows the DC-bus capacitor voltages, V_{c1} and V_{c2}. The use of capacitor voltage unbalance controller in the

control scheme results in a smaller DC-bus capacitor voltage unbalancing problem as shown in Fig. 28, when the rectifier feeds balanced loads.
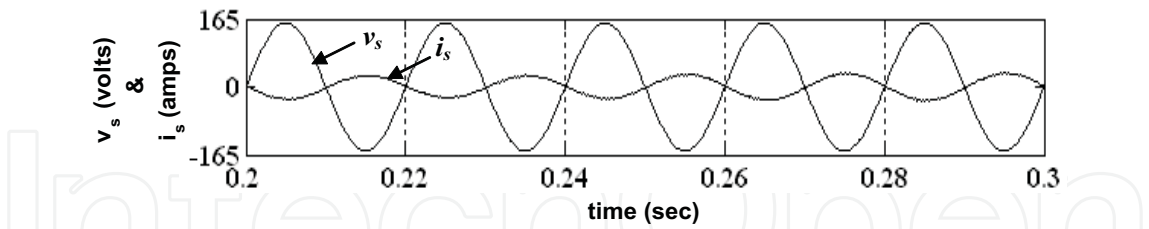
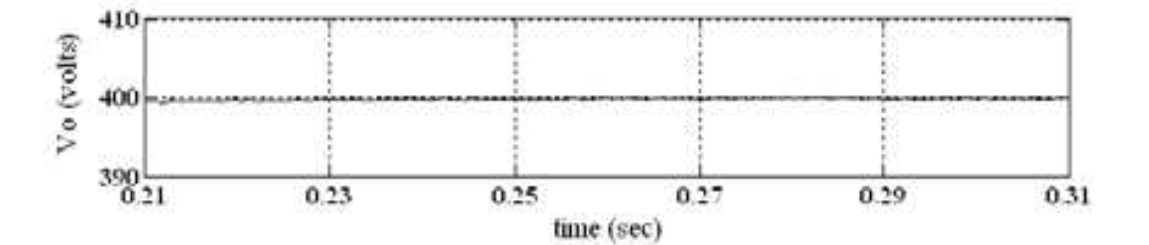Fig. 26. Phase *A* voltage and line-current waveforms for inversion mode of operation
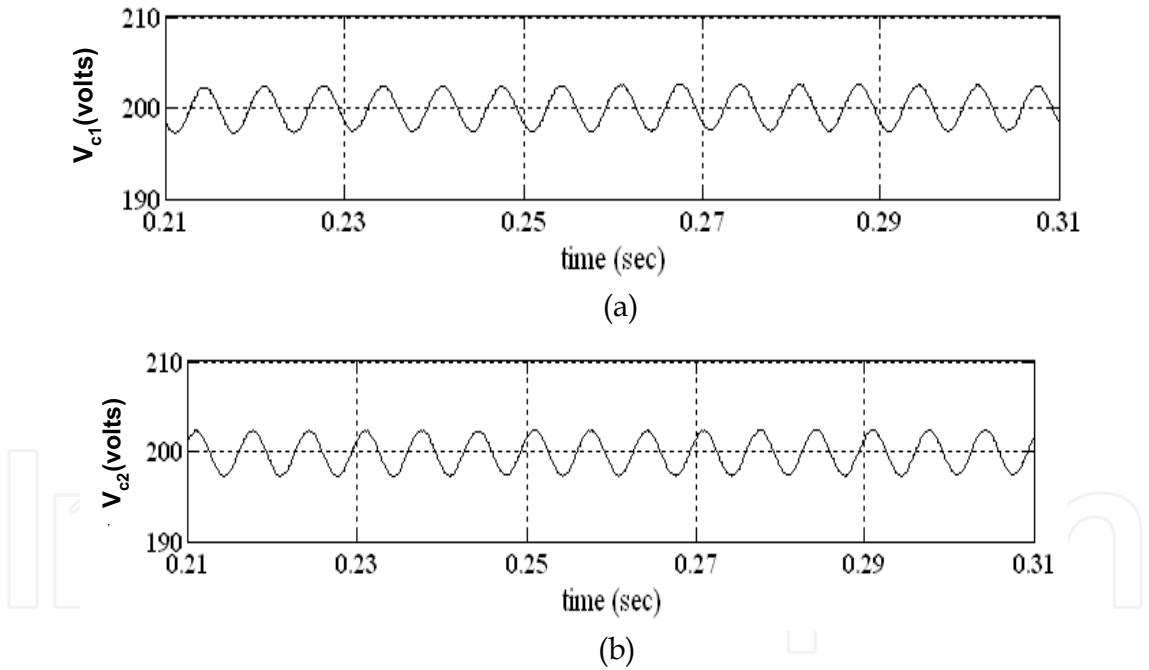
Fig. 27. DC-bus voltage of rectifier

(a)

(b)

Fig. 28. DC-Bus capacitor voltages (a) Voltage across C_1 (b) Voltage across C_2

9. Space vector pulse width modulation (SVPWM)

A standard space vector modulation technique [2] has been used for the three-phase neutral-point clamped bidirectional rectifier of Fig. 20. The basic operating principle of the rectifier employing SVPWM is discussed below.

As shown in Fig. 20, the input terminals of the rectifier *a*, *b* and *c* are connected to the terminals of three-phase source *A*, *B* and *C* through the filter inductances *L*. Each power

switch has a voltage stress of half the DC bus voltage instead of full DC bus voltage in the two-level PFCs. The power switches are commutated with a high switching frequency to generate the PWM voltages v_a', v_b' and v_c'.
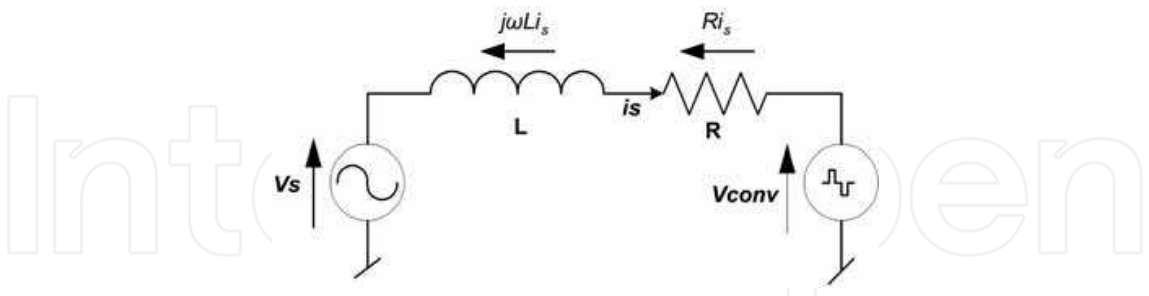

Fig. 29. Single-phase representation of NPC rectifier circuit

Fig. 29 shows a single-phase representation of the three-phase NPC rectifier of the Fig. 20. Again, L and R represent the line inductor. v_s is the source voltage and v_{conv} is the bridge converter voltage controllable from the DC-side. Magnitude of v_{conv} depends on the modulation index and DC voltage level of the converter. The inductors connected between input of the rectifier and supply lines are integral part of the circuit. They provide the boost feature of converter. The line-current, i_s is controlled by voltage drop across the inductance L interconnecting two voltage sources (line and converter). It means that the inductance voltage v_L equals the difference between the line voltage v_s and the converter voltage v_{conv}. Upon controlling the phase angle δ and the amplitude of the converter voltage v_{conv}, the phase and amplitude of the line-current are indirectly controlled. In this way, the average value and sign of DC current is subject to control the active power conducted through the converter. The reactive power can be controlled independently with shift of fundamental harmonic current i_s in respect to voltage v_s.
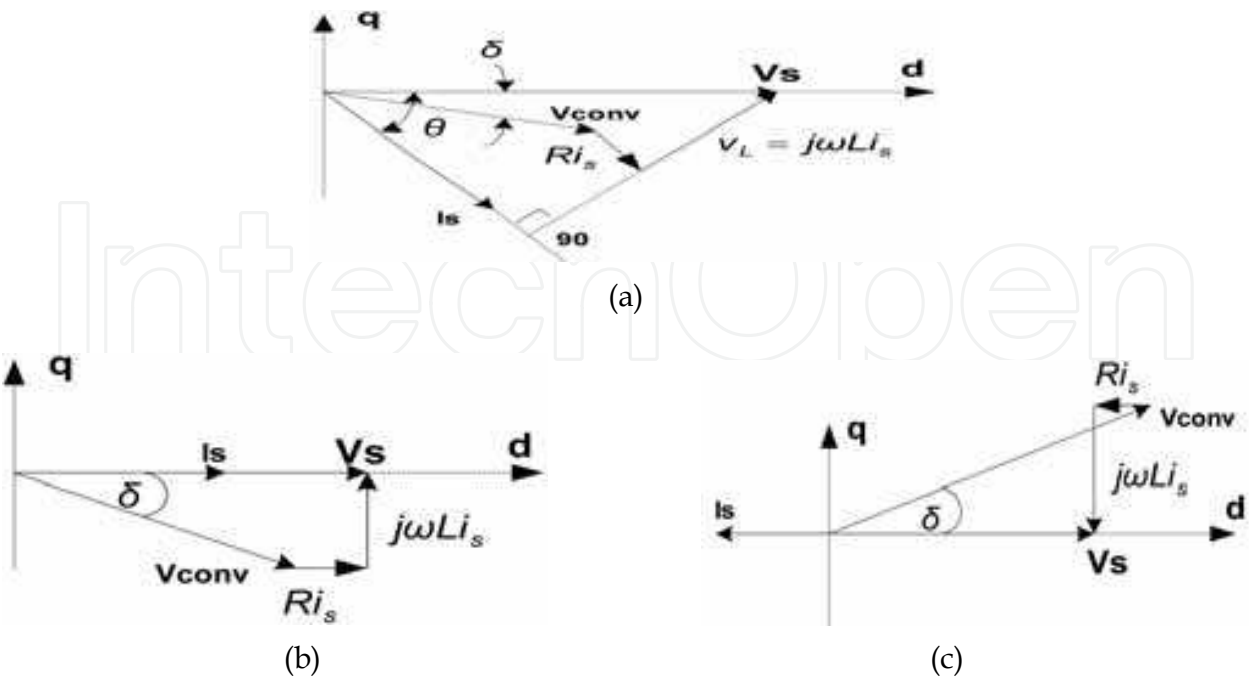

Fig. 30. Phasor diagram of NPC PWM rectifier (a) General phasor diagram, (b) Rectification at unity power factor, (c) Inversion at unity power factor

Fig. 30 presents the general phasor diagram and both rectification and regeneration phasor diagrams when unity power factor operation is required. The figure clearly shows that the voltage vector v_{conv} is higher during the regeneration than the rectification mode. It means that these two modes are not symmetrical.

Now,

$$v_s = v_{conv} + v_L \tag{22}$$

where

$$v_L = L.\frac{di_s}{dt} \tag{23}$$

Assuming v_s to be sinusoidal, the fundamental-frequency component of v_{conv} and supply current i_s can be expressed as phasors v_{conv1} and i_{s1}, respectively (not shown in the phasor diagram). Choosing v_s arbitrarily as the reference phasor $v_s = v_s e^{j0°}$, at line frequency $\omega = 2\pi f$, we can write

$$v_s = v_{conv1} + v_{L1} \tag{24}$$

where

$$v_{L1} = j\omega L i_{s1} \tag{25}$$

Here the resistance R is assumed to be small and hence neglected.

The real power 'P' supplied by the phase A of the three-phase AC source to the converter is given as,

$$P = v_s i_{s1} \cos\theta = \frac{v_s^2}{\omega L}\left(\frac{v_{conv1}}{v_s}\sin\delta\right) \tag{26}$$

since in Fig. 30, $v_{L1}\cos\theta = \omega L i_{s1}\cos\theta = v_{conv1}\sin\delta$ (with v_L, v_{conv} and i_s replaced by their fundamental components as v_{L1}, v_{conv1} and i_{s1}, respectively and $R=0$).

In this phasor diagram, the reactive power 'Q' supplied by phase A of the AC source is positive and can be expressed as,

$$Q = v_s i_{s1} \sin\theta = \frac{v_s^2}{\omega L}\left(1 - \frac{v_{conv1}}{v_s}\cos\delta\right) \tag{27}$$

since in this figure, $v_s - \omega L i_{s1}\sin\theta = v_{conv1}\cos\delta$.

It is worth noting that 'Q' is the sum of the reactive power absorbed by the converter and the reactive power consumed by the inductance L. However, at very high switching frequencies, L can be made to be quite small; thus, Q can be approximated as the reactive power absorbed by the converter. The current i_{s1} can be written as,

$$i_{s1} = \frac{v_s - v_{conv1}}{j\omega L_s} \tag{28}$$

From equations (26) to (28), it is clear that for a given line-voltage, v_s and the chosen inductance L, the desired values of P and Q can be obtained by controlling the magnitude and the phase of v_{conv1}.

In the above general analysis, two cases are of special interest: rectification and inversion at a unity power factor. These two cases are depicted in Fig. 30(b) and Fig. 30(c).

In both cases,

$$v_{conv1} = [v_{s^2} + (\omega L i_{s1})^2]^{1/2} \quad \text{(with } R=0\text{)} \tag{29}$$

Thus, for the desirable magnitude and the direction of power flow as well as Q, the magnitude of v_{conv1} and the phase angle δ with respect to the line voltage v_s must be controlled.
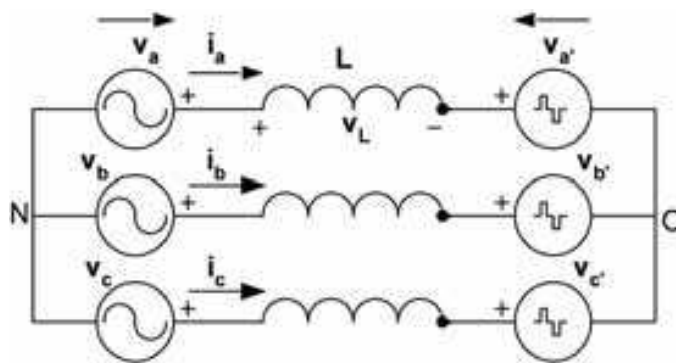
Fig. 31. Equivalent circuit of three-phase NPC rectifier

Now, the equivalent circuit of three-phase NPC rectifier of Fig. 20, as shown in Fig. 31, is considered for following analysis.

The space vectors are defined as below:

$$v = \tfrac{2}{3}\left(v_a + a.v_b + a^2.v_c\right) \tag{30}$$

$$v' = \tfrac{2}{3}\left(v_a' + a.v_b' + a^2.v_c'\right) \tag{31}$$

$$i = \tfrac{2}{3}\left(i_a + a.i_b + a^2.i_C\right) \tag{32}$$

The voltage vector equation can be written as below:

$$v = L.\tfrac{di}{dt} + v' \tag{33}$$

This equation can be expressed in a rotating reference frame (d-q), with the d-axis oriented in the direction of source voltage vector v as depicted in Fig. 32. Thus the equation (33) can be written as,

$$v_d = L.\tfrac{di_d}{dt} - \omega.L.i_q + v_{d'} \tag{34}$$

$$v_q = 0 = L.\tfrac{di_q}{dt} + \omega.L.i_d + v_{q'} \tag{35}$$

where ω is the angular frequency of three-phase voltage and v_d, $v_d{'}$, i_d and v_q, $v_q{'}$, i_q are the components of v, v' and i_s in the d and q-axis respectively.
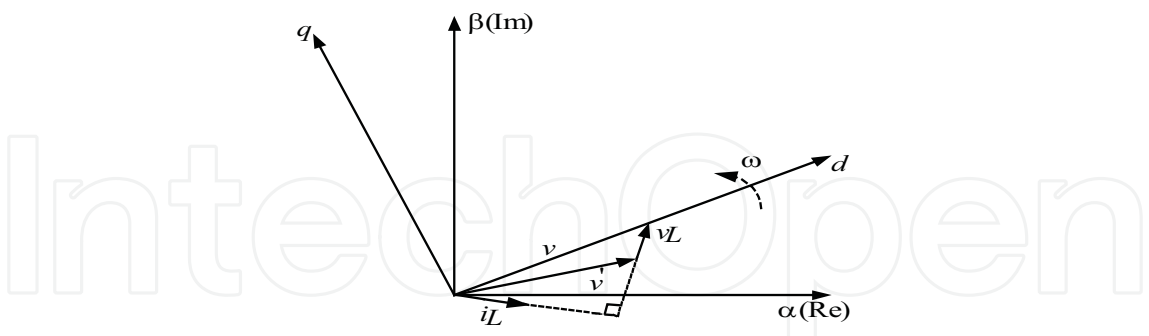

Fig. 32. Vector diagram of SVM-based NPC rectifier

Equations (34) and (35) show that the behaviour of currents i_d and i_q can be controlled by using the voltages $v_d{'}$ and $v_q{'}$ generated by the rectifier. In this way, the active as well as the reactive powers delivered by the mains to rectifier can be controlled.
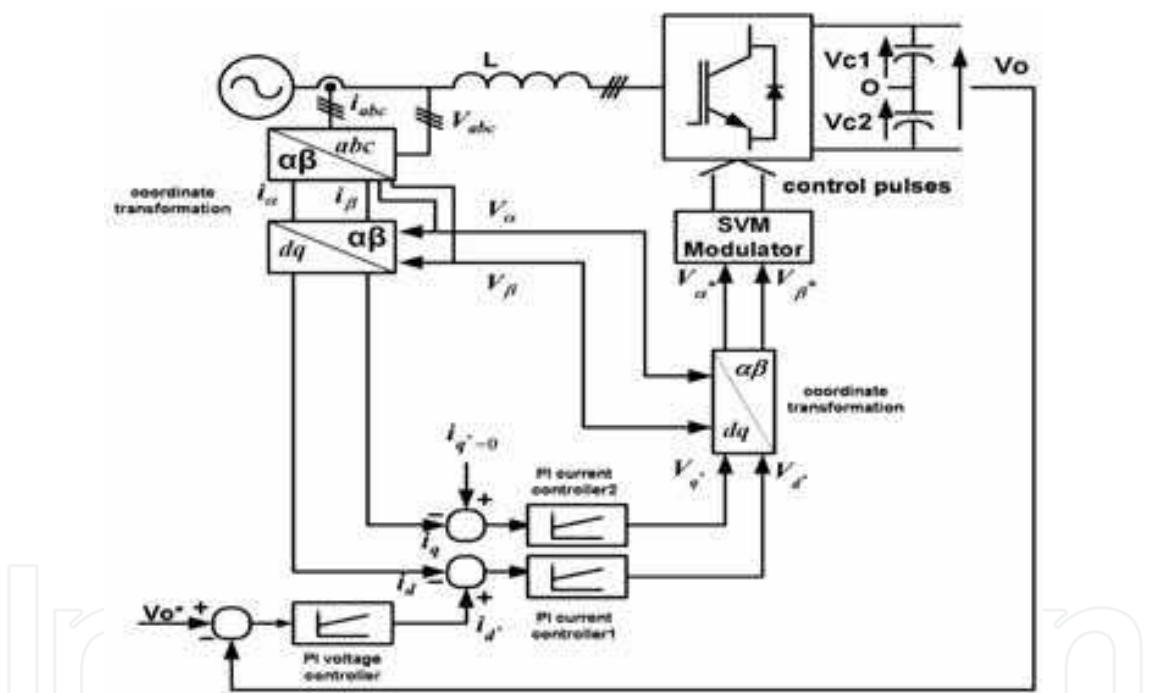
Fig. 33. Block diagram of voltage-oriented control scheme

The control strategy of this rectifier is the same as employed in two-level PWM rectifiers using SVPWM [4]. It is shown in Fig. 33. A PI controller is used to control the converter output voltage V_o. The output of this controller, $i_d{}^*$ is used as reference for an inner closed-loop used to control the direct current i_d. The current in the q-axis, i_q is controlled by a similar loop with reference, $i_q{}^*=0$ to obtain operation with unity power factor. It is to be emphasized that this method only controls the total DC-bus voltage V_o and does not ensure the balance of capacitor voltages V_{c1} and V_{c2}. For proper converter operation, $V_{c1} = V_{c2}$. The current-controllers deliver the reference values for the voltages in the d and q-axis, $V_d{}^*$ and $V_q{}^*$ respectively. By using coordinates transformation, we obtain $V_a{}^*$ and $V_\beta{}^*$ in the stationary reference frame (a, β). Voltages $V_a{}^*$ and $V_\beta{}^*$ are used to derive the reference command input

voltage V^* and its angle θ. These are delivered as inputs to the space vector modulator which generates the control pulses for converter switches using the 'Nearest Three Vector' (NTV) approach of SVM.

Applying the definition of equation (31) to all the 27 possible conduction states of power semiconductors, the converter generates 19 different space vectors as shown in Fig. 34(a). This figure also depicts the commutation states used to generate each space vector. It can be proved that the neutral current will flow through point o in all the states except the zero switching states located at the origin and large voltage vectors located at the outer hexagon corner states as shown in this figure. The complex plane is divided into six sectors and 24 triangles with four triangles (also called regions) in each sector. Fig. 34(b) shows the 'sector 1' triangle formed by voltage vectors V_o, V_7 and V_9. Assuming the command voltage vector V^* to be in region R_3, the following equations should be satisfied for SVPWM:

$$V_1 T_a + V_8 T_b + V_2 T_c = V * T_s / 2 \tag{36}$$

$$T_a + T_b + T_c = T_s / 2 \tag{37}$$

where V_1, V_8 and V_2 are the space vectors at the corners of region R_3, T_a, T_b, and T_c are the respective vector time intervals of these vectors and T_s is the sampling time.

Taking *sector 1* as the reference, the analytical time expressions for T_a, T_b, and T_c for all the regions can be derived and are written as:

$$\text{Region-1:} \quad \begin{aligned} T_a &= 2kT_s \sin\left(\frac{\pi}{3} - \theta\right) \\ T_b &= T_s\left[1 - 2k\sin\left(\theta + \frac{\pi}{3}\right)\right] \\ T_c &= 2kT_s \sin\theta \end{aligned}$$

$$\text{Region-2:} \quad \begin{aligned} T_a &= 2T_s\left[1 - k\sin\left(\theta + \frac{\pi}{3}\right)\right] \\ T_b &= 2kT_s \sin\theta \\ T_c &= T_s\left[2k\sin\left(\frac{\pi}{3} - \theta\right) - 1\right] \end{aligned}$$

$$\text{Region-3:} \quad \begin{aligned} T_a &= T_s[1 - 2k\sin\theta] \\ T_b &= T_s\left[2k\sin\left(\theta + \frac{\pi}{3}\right) - 1\right] \\ T_c &= T\left[1 + 2k\sin\left(\theta - \frac{\pi}{3}\right)\right] \end{aligned}$$

$$\text{Region-4:} \quad \begin{aligned} T_a &= T_s[2k\sin\theta - 1] \\ T_b &= 2kT_s \sin\left(\frac{\pi}{3} - \theta\right) \\ T_c &= 2T_s\left[1 - k\sin\left(\theta + \frac{\pi}{3}\right)\right] \end{aligned} \tag{38}$$

where θ is the command voltage vector angle and $k = 2/\sqrt{3}\,(V^*/V_0)$, V^* = command voltage vector and V_o = DC-bus voltage of the rectifier. The above time intervals are distributed appropriately so as to generate symmetrical PWM pulses for the rectifier
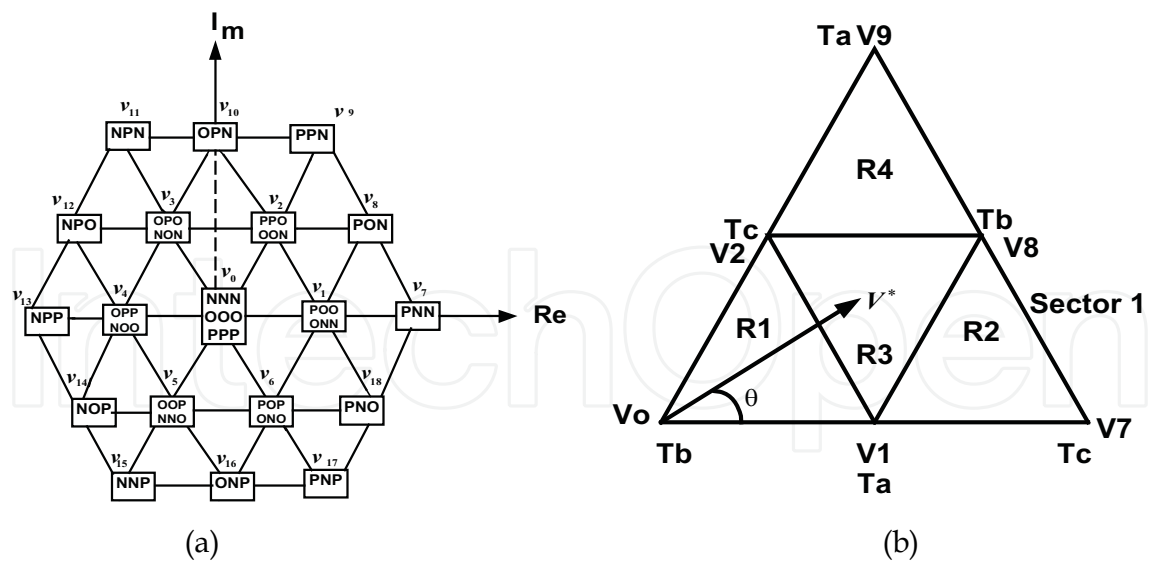
Fig. 34. (a) Space vector diagram showing all the 27 switching states (b) Sector *1* space vectors with switching times

10. Performance evaluation

The performance of the SVPWM-based NPC converter is evaluated under ideal mains conditions and various performance indices are obtained after exhaustive simulations. The same system parameters as used in the SPWM-based converter (given in Table 4) are employed for the simulation of rectifier.

The steady-state performance of rectifier is evaluated with a constant source voltage and fixed load. Before the evaluation of performance of the rectifier, it is operated on three-phase supply without any control algorithm being implemented for its control. Fig. 35 shows the phase *A* source voltage and line-current waveforms of the converter when operated on an R-L load without the SVPWM algorithm. The line current drawn by the rectifier is highly distorted and rich in harmonics. As shown in Fig. 36, the line-current THD is 20.21% which is unacceptably large. Now, the performance of the rectifier is evaluated by applying the control algorithm for control of load voltage and wave shaping of source current drawn by rectifier from the mains. Fig. 37 shows phase *A* source voltage and line current waveforms in the rectification mode of operation. The frequency spectrum of line-current is shown in Fig. 38. It shows a line-current THD of only 1.45%, which is less than half the THD of source current obtained in SPWM technique. Fig. 39 shows the voltage generated at the rectifier input terminals after the SVPWM algorithm is applied. The source voltage and line-current waveforms of the converter in the inversion mode of operation are shown in Fig. 40. The line current is still free from harmonic pollution and has a THD of just 1.60% as shown in the frequency spectrum of current in Fig. 41. The transition from rectification mode to inversion mode of operation is shown in Fig. 42. It takes about two cycles for the converter to completely transition from rectification to inversion mode of operation. The load voltage waveform is shown in Fig. 43. It is observed that the load voltage is regulated with a negligible ripple factor of only 0.55 volt, which is a highly desirable feature in most of the applications. Fig. 44 shows the DC-bus capacitor voltages, V_{c1} and V_{c2}. Since the control scheme does not consider the capacitor voltage balancing issue, a somewhat higher capacitor voltage unbalance is produced. It is found that the SVPWM-based rectifier gives a

better performance than that of SPWM-based rectifier at the same switching frequency. In other words, for the same performance, the SVPWM-based rectifier can be operated at a reduced switching frequency which reduces the switching stress of the devices and also the power losses of the converter. Moreover, there is no need of synchronizing the modulating and carrier waves and a better utilization of DC-link voltage is possible. The space vector PWM has a large number of redundant switching states which can be utilized for the balancing of DC-bus capacitor voltages. In view of these facts, the space vector PWM is preferred over sinusoidal PWM modulation strategy.
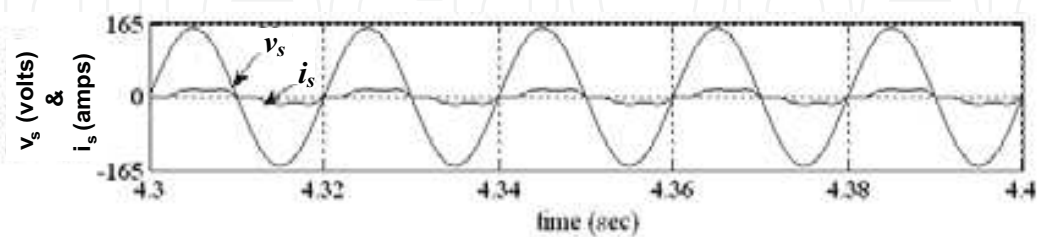
Fig. 35. Phase *A* source voltage and source current waveforms without control
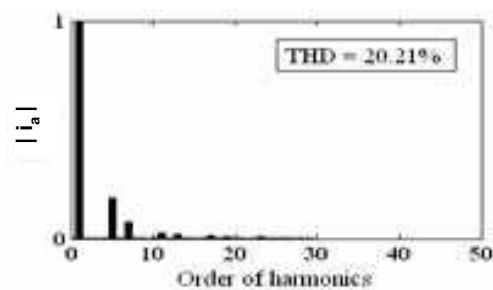
Fig. 36. Frequency spectrum of source current
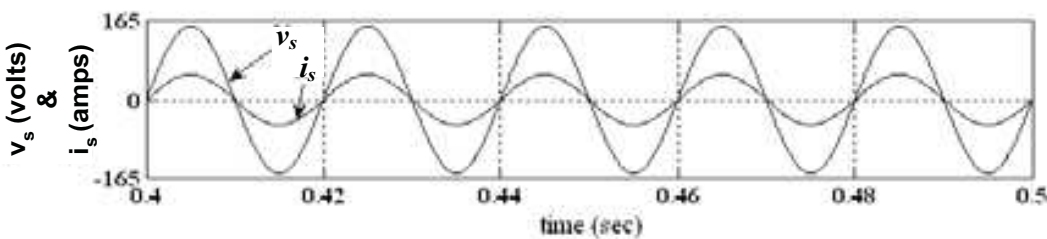
Fig. 37. Phase *A* source voltage and source current waveforms for rectification mode of operation
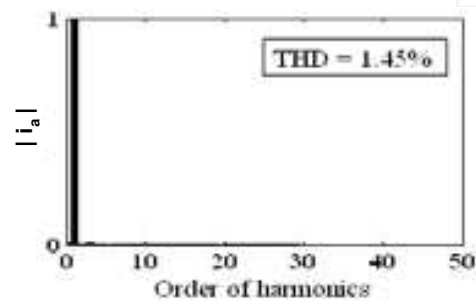

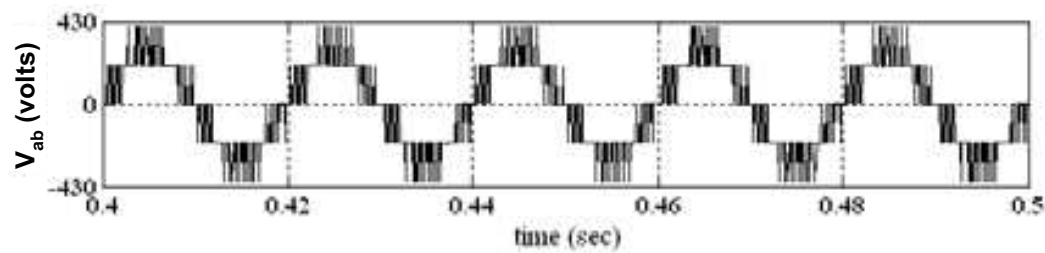Fig. 38. Frequency spectrum of source current

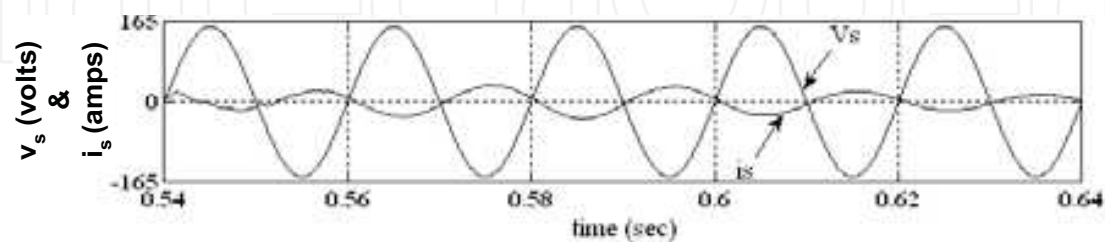Fig. 39. Voltage reflected at the rectifier input terminals

Fig. 40. Phase *A* source voltage and source current waveforms in inversion mode of operation
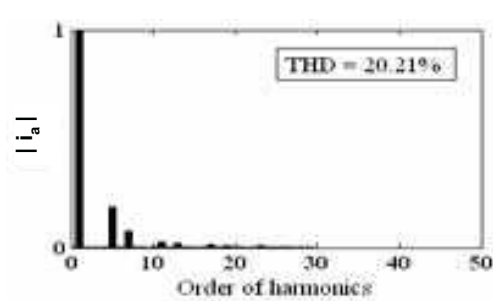

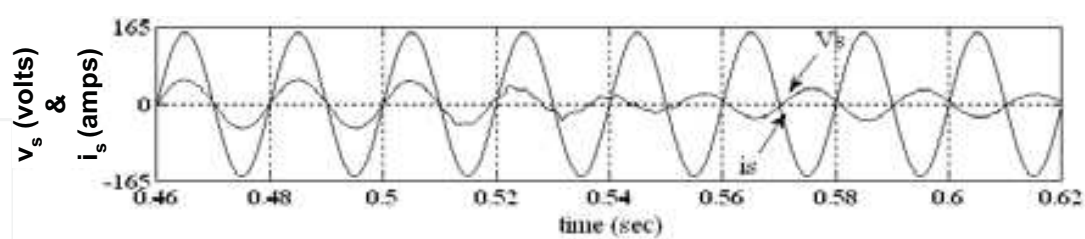Fig. 41. Frequency spectrum of source current in inversion mode

Fig. 42. Phase *A* voltage and line-current waveforms for transition from rectification to inversion mode (Rectification-to-Inversion transition starts at t = 0.51 sec.)
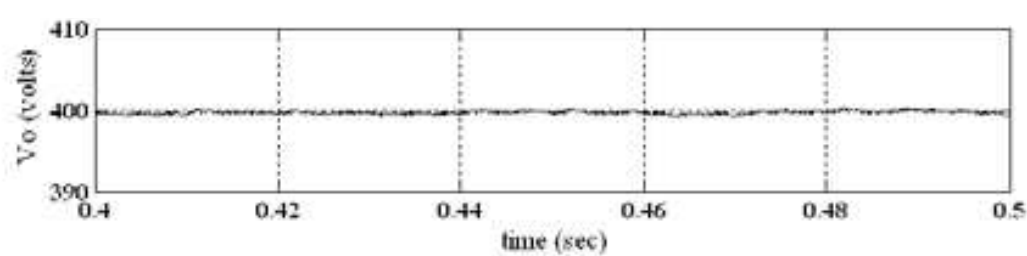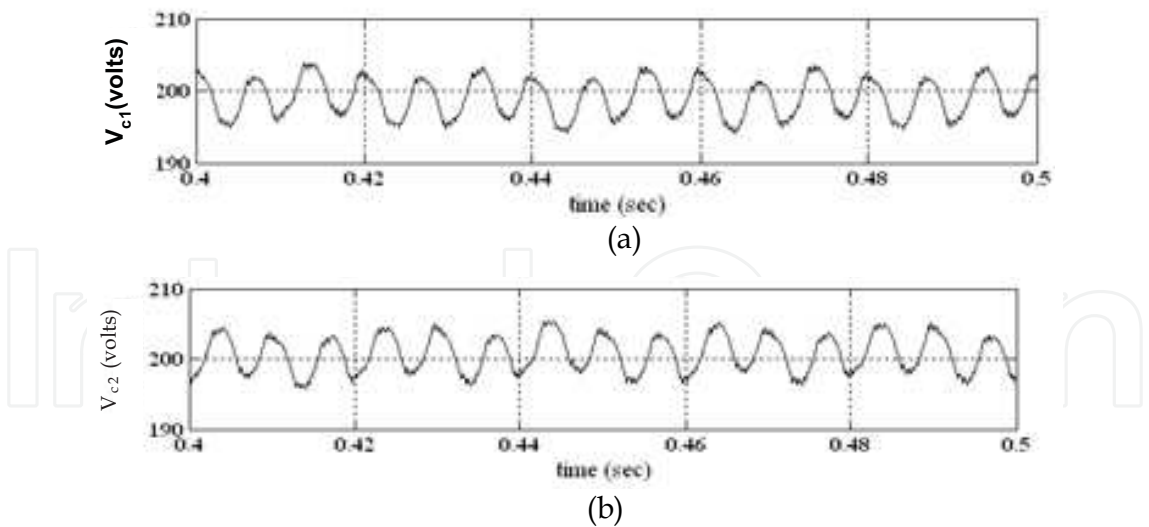

Fig. 43. Load voltage waveform

(a)

(b)

Fig. 44. DC-Bus capacitor voltages (a) Voltage across C_1 (b) Voltage across C_2

11. Experimental validation

A laboratory prototype of the three-phase, improved power quality neutral-point clamped rectifier is developed by integrating the power circuit, the control hardware and the DSP and tested in the laboratory to experimentally validate the simulation results. The performance of the system is investigated experimentally under steady-state. The system parameters selected for the experimental verification are given in Table – 5.

System Parameters	
Supply-side parameters	**Load-side parameters**
Supply voltage: 40 volts (peak), 50 Hz	Load: $R_o = 15\ \Omega$, $L_o = 5$ mH
Boost Inductor: L = 4.5 mH, R = 0.4 Ω	DC-Bus capacitors: $C_1 = C_2 = 4700\ \mu F$
Reference DC voltage: $V_o{}^* = 100$ volts	
Sampling frequency, $f_s = 5$ kHz	

Table 5. System parameters for Experimentation

For real-time implementation of SVPWM control algorithm, DSP *DS1104* of dSPACE has been used. Fig. 45 shows the block diagram of laboratory prototype of DSP-based real-time implementation of a three-level improved power quality converter.

The DSP *DS1104* R&D Controller Board of dSPACE is a standard board that can be plugged into a PCI slot of a PC. The DS1104 is specifically designed for the development of high-speed multivariable digital controllers and real-time simulations in various fields. It is a complete real-time control system based on a 603 PowerPC floating-point processor running at 250 MHz. For advanced I/O purposes, the board includes a slave-DSP subsystem based on the TMS320F240 DSP microcontroller. For the purposes of rapid control prototyping (RCP), specific interface connectors and connector panels provide easy access to all input and output signals of the board. Thus, DS1104 R&D Controller Board is the ideal hardware for the dSPACE prototyper development system for cost-sensitive RCP applications. It is used for the real-time simulation and implementation of the control algorithm in real-time. In real-time simulation, the real plant (converter) is controlled by the controller (SVPWM modulator) that is simulated in real time. This technique is called rapid control prototyping (RCP).
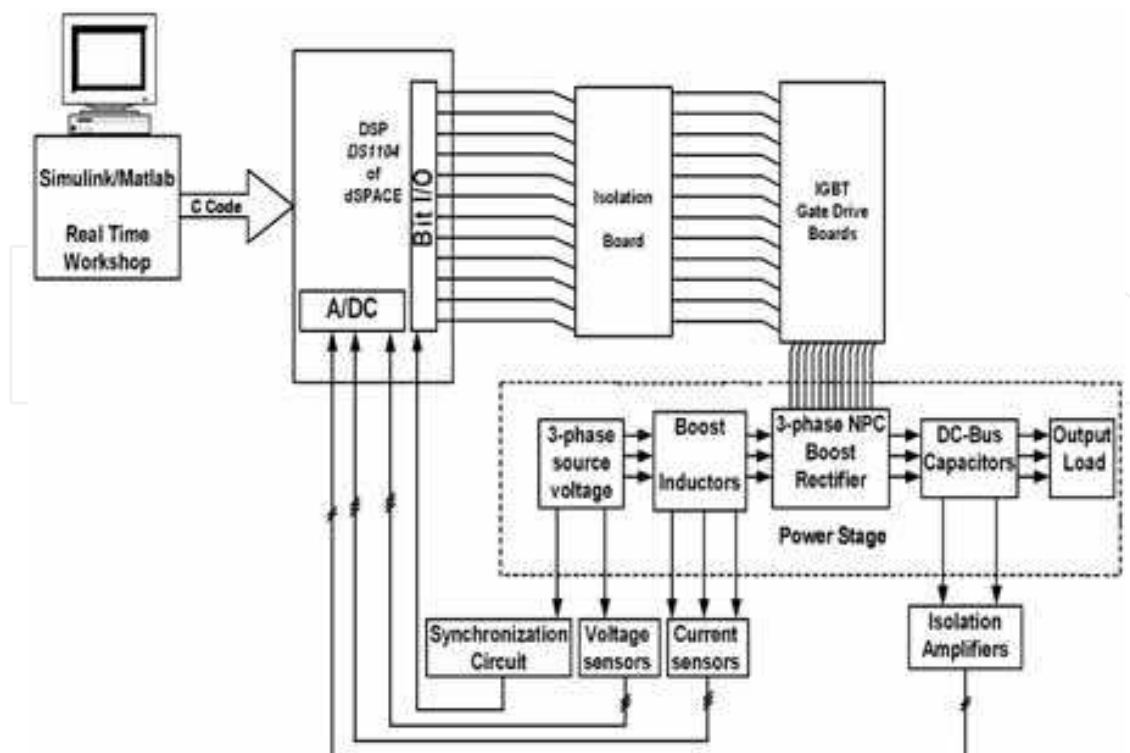
Fig. 45. Block diagram of DSP-Based NPC Rectifier Implementation

The major feature of real-time simulation is that the simulation has to be carried out as quickly as the real system would actually run, thus allowing to combine the simulation and the converter (real plant). The sensed AC and DC voltages and source currents are fed to the dSPACE board via the available ADC channels on its connector panel. In order to add an I/O block (like ADCs and master bit I/Os in this case) to the simulink model, the required block is dragged from the dSPACE I/O library and dropped into the simulink model of the SVPWM modulator. In fact, adding a dSPACE I/O block to a simulink model is almost like adding any simulink block to the model. In this case, twelve master bit I/Os, configured in the output mode, are connected to the model for outputting the twelve gating signals to the IGBTs of NPC rectifier bridge. In addition, eight ADCs are connected to the model for inputting the three sensed AC voltage signals, three source current signals and two DC bus capacitor voltages to the DSP hardware. These sensed signals are used for processing in the space vector PWM modulation algorithm. Because real-time simulation is such a vital aspect for control engineering, the same is true for the automatic generation of real-time code, which can be implemented on the hardware. For dSPACE systems, Real-Time Interface (RTI) carries out this linking function. Together with Real-Time Workshop from the MathWorks, it automatically generates the real-time code from simulink models and implements this code on dSPACE real-time hardware. This saves the time and effort twice as there is no need to manually convert the simulink model into another language such as C and we do not need to be concerned about a real-time program frame and I/O function calls, or about implementing and downloading the code onto the dSPACE hardware. RTI carries out these steps and we just need to add the required dSPACE blocks (I/O interfaces, etc.) to our simulink model. In other words, RTI is the interface between Simulink and various dSPACE platforms. It is basically the implementation software for single-board hardware and connects the simulink control model to the I/O of the board. In the present case, the optimized C-code of the simulink model of control algorithm is automatically

generated by the Real-Time Workshop of MATLAB in conjunction with dSPACE's Real-Time Interface (RTI). The generated code is then automatically downloaded into the dSPACE hardware where it is implemented in real-time and the gating pulses are generated. The gating pulses for the power switches of converter are outputted via the master-bit I/Os available on the dSPACE board. The CLP1104 Connector/LED Combi panel provides easy-to-use connections between DS1104 board and the devices to be connected to it. The panel also provides an array of LEDs indicating the states of digital signals (gating pulses). The gating pulses are fed to various IGBT driver circuits via the opto-isolation circuit boards.
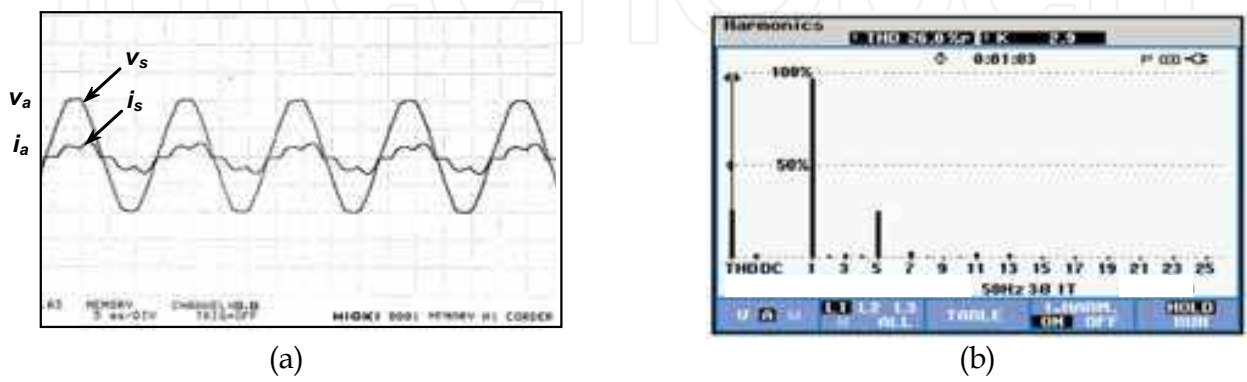

(a)   (b)

Fig. 46. (a) Phase *A* voltage and line-current waveforms before implementing SVPWM algorithm X-axis: time – 5 mS/div. Y-axis: v_a – 20 volts/div, i_a – 10A/div. (b) Frequency spectrum of phase *A* line-current
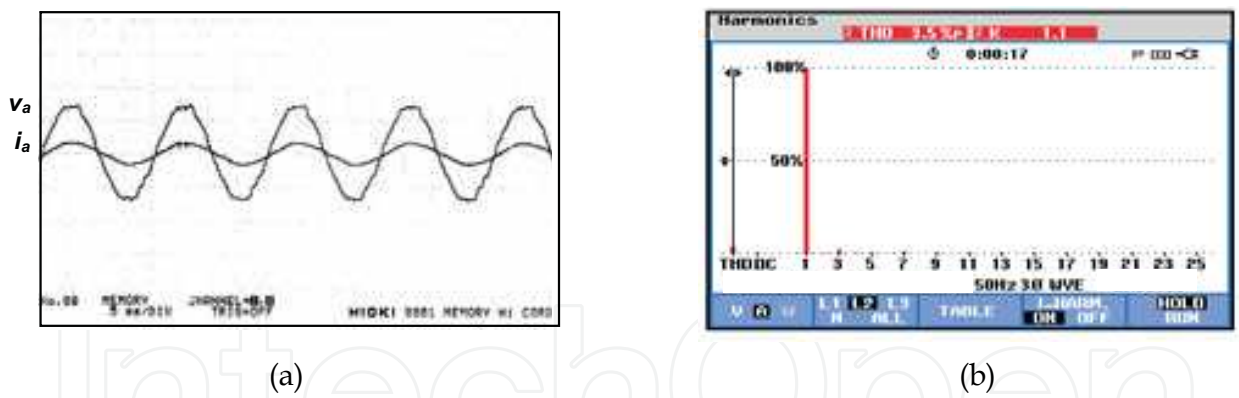

(a)   (b)

Fig. 47. (a) Phase *A* voltage and line-current waveforms after implementing SVPWM algorithm X-axis: time – 5 mS/div. Y-axis: v_a – 25 volts/div, i_a – 10A/div. (b) Frequency spectrum of phase *A* line-current

Fig. 46(a) shows the phase-*A* source voltage and line current drawn by the rectifier with an R-L load before the implementation of the space vector PWM algorithm. It is observed that the current drawn by the rectifier is highly distorted in nature and rich in harmonics. This is shown in the frequency spectrum of phase-*A* line current, as depicted in Fig. 46(b). This figure shows a line-current THD of 26%. After the implementation of the SVPWM control algorithm using dSPACE, the line current drawn by the rectifier becomes nearly sinusoidal in nature, as shown in Fig. 47(a). The current is drawn by the rectifier at unity power factor. This makes the rectifier work as a linear load in the system, causing almost no distortion of line-currents and no reactive power flow. The line-current THD is reduced drastically from

an alarmingly large value of 26% to a mere 3.5% as shown in the frequency spectrum of line-current in Fig. 47(b). The THD is below the 5% limit prescribed by IEEE-519 standards.

Fig. 48 shows the voltage generated between the input terminals of the rectifier. Fig. 49(a) shows the phase-*A* voltage and current waveforms when the converter operates in inversion mode, thus regenerating power back to source. Thus the bidirectional neutral-point clamped converter is capable of operating in both the rectification as well as inversion modes. It is worth noting that the space vector control algorithm keeps the line currents sinusoidal. It is clear from the frequency spectrum of source current as shown in Fig. 49(b). The source current THD is 4.8% which is below the imposed limit of 5% by IEEE 519.
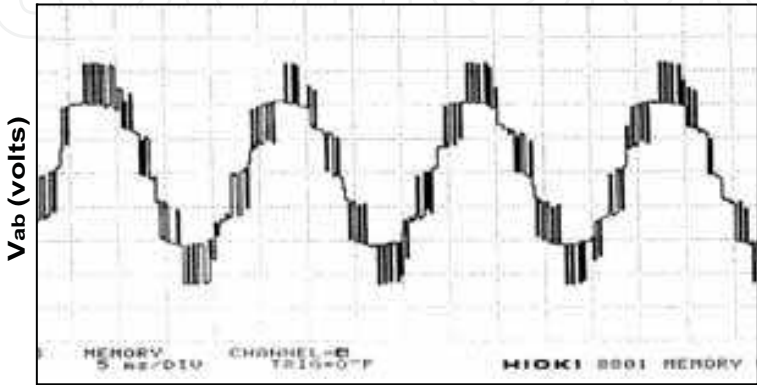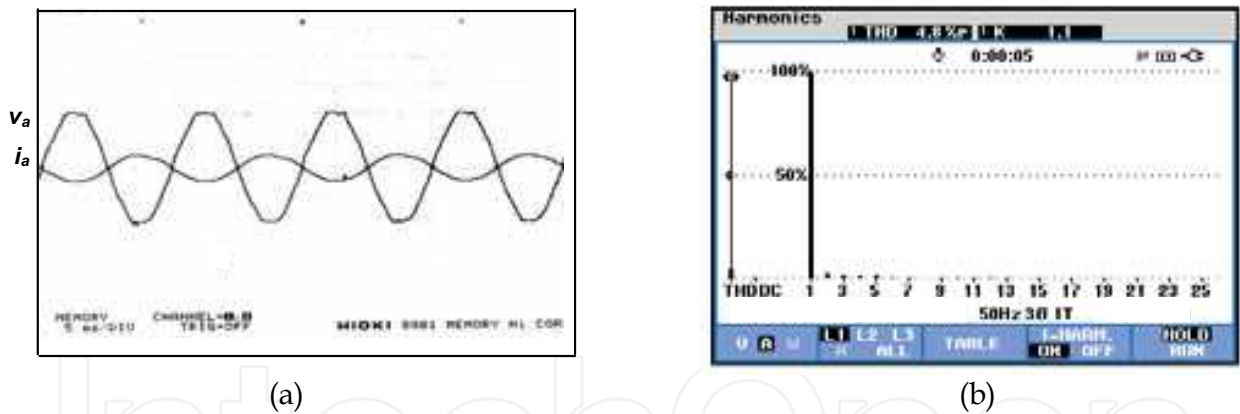

Fig. 48. Voltage at the rectifier input terminals

(a)   (b)

Fig. 49. (a) Phase *A* voltage and current waveforms in inversion mode X-axis: time – 5 mS/div. Y-axis: v_a – 20 volts/div & i_a – 10 A/div. (b) Frequency spectrum of source current

Fig. 50 shows the DC-bus capacitor voltages of the converter. Fig. 51 shows the load voltage (DC-bus voltage) impressed across the load. It is observed that the load voltage is regulated at the desired reference value of 100 volts. Thus the experimental waveforms of source current and load voltage validate the simulation results obtained. Various harmonic components present in the source current before and after the implementation of SVPWM control algorithm are shown in Tables 6 and 7. Corresponding harmonic components obtained by simulation for almost similar conditions are also presented for comparison.

Thus summarising, the performance of space-vector PWM based neutral-point clamped rectifier model has been thoroughly investigated and the simulation results have been experimentally validated. It is found that the converter operation gives good power quality both at the line-side and load-side of the converter like sinusoidal source currents at nearly

unity power factor, reduced line-current THD and regulated and reduced rippled DC bus voltage. The given converter finds tremendous applications in various industrial applications as it elegantly addresses the burning power quality issues created by the use of conventional diode bridge rectifiers and line-commutated converters.
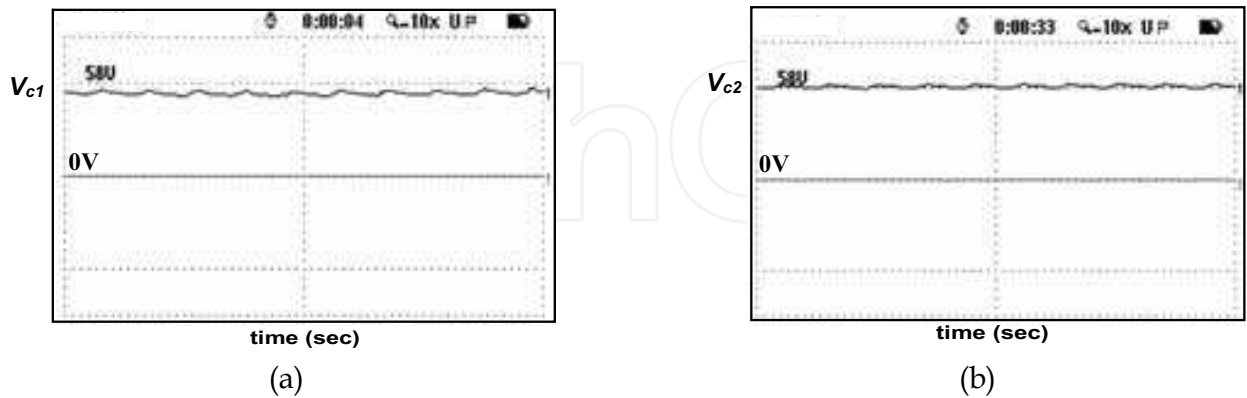

(a)   (b)

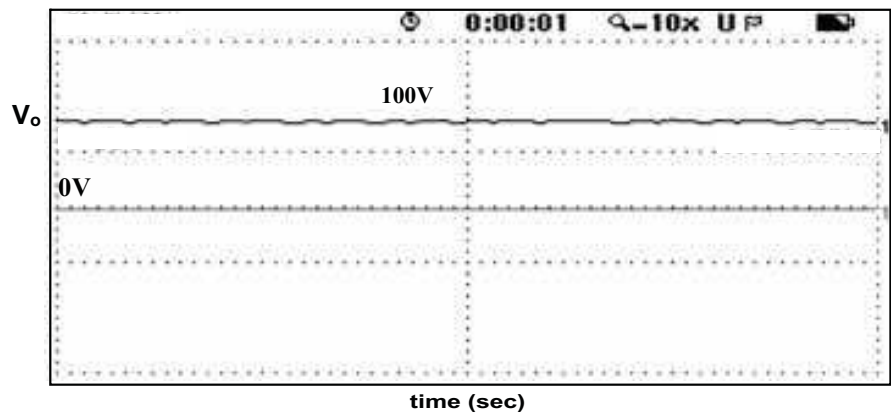Fig. 50. DC–Bus Capacitor Voltages (a) Voltage across capacitor C_1 (b) Voltage across capacitor C_2

Fig. 51. DC–Bus (Load) Voltage

Order of harmonics	Harmonic components (% of fundamental) (Source current)	
	Simulation	Experimental
3	0.01	1.9
5	23.47	25.3
7	7.27	3.2
9	0.0	0.2
11	3.78	2.8
13	2.90	2.3
15	0.0	0.4
17	1.30	2.1
19	1.07	2.07
% THD	25.13%	26%

Table 6. Harmonic components present in source current without applying SVPWM algorithm

Order of harmonics	Harmonic components (% of fundamental) (source current)	
	Simulation	Experimental
3	0.88	1.09
5	0.28	0.25
7	0.09	0.85
9	0.3	0.62
11	0.11	0.12
13	0.16	0.38
15	0.23	0.20
17	0.07	0.15
19	0.08	0.09
% THD	1.45%	3.5%

Table 7. Harmonic components present in source current after applying SVPWM algorithm

12. References

[1] Akagi H., "New Trends in active filters for power conditioning," IEEE Trans. on Industry Applications, vol. 32, Nov./Dec. 1996, pp. 1312-1322.

[2] Bendre A., Krstic S., Meer J. V., and Venkataramanan G., "Comparative Evaluation of Modulation Algorithms for Neutral-Point-Clamped Converters", IEEE Trans. on Industry Applications, vol. 41, no. 2, March/April 2005, pp. 634-643.

[3] Carlton D. and Dunford W. G., "Multilevel, unidirectional AC-DC converters, a cost effective alternative to bi-directional converters," in Proc. IEEE PESC'01, 2001, pp. 1911-1917.

[4] Dixon J. W., "Boost type PWM rectifiers for high power applications," Ph.D dissertation, Dept. Elect. Comput. Eng., McGill Univ., Montreal, QC, Canada, Jun. 1988.

[5] El-Habrouk M., Darwish M. K., and Mehta P., "Active power filters: a review", Proc. IEE-Electric Power Applications, vol. 147, pp. 493-513, Sept. 2000.

[6] Fukuda S. and Hasegawa H., "Current source rectifier/inverter system with sinusoidal currents," in Conf. Rec. IEEE-IAS Annual Meeting, 1988, pp. 909-914.

[7] Fuld B., Kern S., and Ridley R., "A combined buck and boost power-factor-controller for three-phase input," in Power Electronics and Applications, European Conference, Sep. 1993.

[8] Groben T., Menzel E., and Enslin J. H. R., "Three-phase buck active rectifier with power factor correction and low EMI," Proc. IEE-Electric Power Applications., vol. 146, no. 6, pp. 591-596, Nov. 1999.

[9] Hengchun Mao, Fred C. Y. Lee, Boroyevich Dushan, and Silva Hiti, "Review of high-performance three-phase power-factor correction circuits," IEEE Trans. on Industrial Electronics, vol. 44, no. 4, August 1997, pp.437-446.

[10] IEEE Recommended Practices and Requirements for Harmonics Control in Electric Power Systems, IEEE std. 519, 1992.

[11] Jain S., Agarwal P., and Gupta H. O., "Design, simulation and experimental investigations on a shunt active power filter for harmonics and reactive power compensation", Electric Power Components and Systems, vol. 32, no. 7, July 2003.

[12] Kolar J. W., Ertl. H., And Zach F. C., "A novel single-switch three-phase ac-dc buck-boost converter with high-quality input current waveforms and isolated dc

output," in Proc. of 15th International Telecommunications Energy Conference, Paris, vol. 2, 1993, pp. 407-414.

[13] Kolar J. W., Ertl. H., and Zach F. C., "A novel three-phase single-switch discontinuous-mode AC-DC buck-boost converter with high quality input current waveforms and isolated output," IEEE Trans. on Power Electronics, vol. 9, Mar. 1994, pp. 160-172.

[14] Konishi Y., Arai N., Kousaka K., and Kumagai S., "A large capacity current source PWM converter with sinusoidal inputs and high power factor," in Proc. IEEE PESC'92 1992, pp. 1361-1367.

[15] Lai J. S. and Peng F. Z., "Multilevel converters: A New Breed of Power Converters", IEEE Trans. on Industry Application, vol. IA-32, No. 3, May/June 1996, pp. 509-517.

[16] Mahfouz A., Holtz J., and El-Tobshy A., "Development of an integrated high voltage 3-level converter-inverter system with sinusoidal input-output for feeding 3-phase induction motors," Power Electronics and Applications, Fifth European Conference, vol. 4, Sep. 1993, pp. 134-139.

[17] Marchesoni M. and Tenca P., "Diode-clamped multilevel converters: A practicable way to balance dc-link voltages," IEEE Trans. on Industrial Electronics, vol. 49, no. 4, August 2002.

[18] Midavaine H., Moigne P. L., and Bartholomeus P., "Multilevel three-phase rectifier with sinusoidal input currents," in Proc. IEEE PESC'96, 1996, pp. 1595-1599.

[19] Omedi T. J. and Barlik R., "Three-phase AC-DC unidirectional PWM rectifier topologies - selected properties and critical evaluation", in IEEE ISIE'96, 1996, pp. 784-789.

[20] Ridriguez J. Rodriguez D., Silva C., and Wiechmann E., "A simple Neutral Point Control for Three-Level PWM Rectifiers", European Power Electronics Conference, EPE'99, 1999, pp. 1-8.

[21] Sinha G. and Lipo T. A., "A four-level rectifier-inverter system for drive applications," IEEE Industry Applications Magazine, vol. 4, Jan./Feb. 1998, pp. 66-74.

[22] Singh B., Al. Haddad K., and Chandra A., "A review of active filters for power quality improvement," IEEE Trans. on Industrial Electronics, vol. 46, Oct. 1999, pp. 960-971.

[23] Singh B., Singh B. N., Chandra A., Al-Haddad K., Pandey A., and Kothari D. P., "A Review of Three-Phase Improved Power Quality AC-DC Converters", IEEE Trans. on Industrial Electronics, vol. 51, No. 3, June 2004, pp. 641-660.

[24] Tamai S., Koyama M., Fujii T., Mizoguchi S. and Kawabata T., "3 level GTO converter-inverter pair system for large capacity induction motor drive," in Conf. Power Electronics and Applications, 1993, pp. 45-50.

[25] Xu L. and Agelidis V. G., "A flying capacitor multilevel PWM converter based UPFC," in Proc. IEEE PESC'01, 2001, pp. 1905-1910.

[26] Yacoubi L., Al-Haddad K., Fnaiech F., and Dessaint L. A., "A DSP-Based Implementation of a New Nonlinear Control for a Three-Phase Neutral Point Clamped Boost Rectifier Prototype," IEEE Trans. on Industrial Electronics, vol. 52, No. 1, Feb. 2005, pp. 197-205.

[27] Zargari N. R. and Joos G., "A current controlled current-source type unity power factor PWM rectifier," in Conf. Rec. IEEE-IAS Annual Meeting, 1993, pp. 793-799.

[28] Zhang R. and Lee F. C., "Optimum PWM pattern for a three-phase boost DCM PFC rectifier", in Proc. IEEE APEC'97, 1997, pp. 895-901.
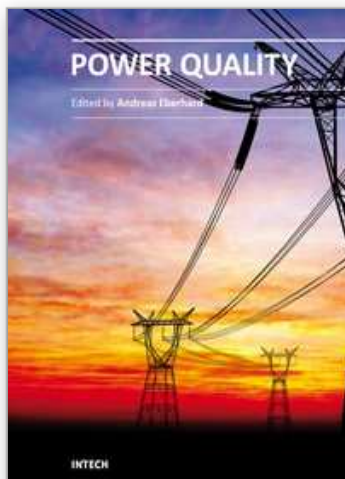
Power Quality

Edited by Mr Andreas Eberhard

Almost all experts are in agreement - although we will see an improvement in metering and control of the power flow, Power Quality will suffer. This book will give an overview of how power quality might impact our lives today and tomorrow, introduce new ways to monitor power quality and inform us about interesting possibilities to mitigate power quality problems.

How to reference

In order to correctly reference this scholarly work, feel free to copy and paste the following:

Abdul Hamid Bhat and Pramod Agarwal (2011). Improved Power Quality AC/DC Converters, Power Quality, Mr Andreas Eberhard (Ed.), ISBN: 978-953-307-180-0, InTech, Available from:
http://www.intechopen.com/books/power-quality/improved-power-quality-ac-dc-converters

INTECH

open science | open minds